3498-1-F

ANALOG COMPUTER INVESTIGATION OF A BOUNDARY-LAYER-CONTROL SYSTEM

MARGARET M. SPENCER

PAUL S. FANCHER

January 1960

ANALOG COMPUTER LABORATORY

Willow Run Laboratories

THE UNIVERSITY OF MICHIGAN

Ann Arbor, Michigan

The work described herein was done for Continental Aviation and Engineering Corporation under Project No. 026-03457. This project was established under an Air Force prime contract, AF 33(600)-38666. This report was written under Continental Aviation and Engineering Corporation Project No. 045-03498.

CONTENTS

FIGURES

TABLES

SYMBOLS

Symbol	Definition	Units
A_L	Effective area of the leakage path	$in.^2$
A_M	Combined area of all exhaust orifices	$in.^2$
A_3	Cross-sectional area of the duct	$in.^2$
B	Magnitude of coulomb friction	lb
F_o	Spring force when x is zero	lb
H_o	Spring force when y is zero	lb
Hp_T	Horsepower from the power turbine to drive the compressor	Hp
K_f	Viscous damping coefficient	lb-sec/in.
N	Compressor rotor speed	RPM
P_1	Total compressor inlet pressure, pounds per square inch, absolute	psia
P_2	The compressor inlet static pressure and the total pressure in chamber 2	psia
P_3	Total compressor outlet pressure	psia
P_A	Total pressure in chamber A	psia
P_B	Total pressure in chamber B	psia
P_C	Total pressure in chamber C	psia
P_M	Total pressure in the manifold	psia
T_1	Temperature of the atmosphere	^oK
T_3	Temperature of the compressor outlet air	^oK
T_A	Temperature in chamber A	^oK
T_B	Temperature in chamber B	^oK
T_C	Temperature in chamber C	^oK
T_M	Temperature in the manifold	^oK
V_A	Volume of chamber A	$in.^3$
V_B	Volume of chamber B	$in.^3$
V_C	Volume of chamber C	$in.^3$
W_a	Air-flow rate out of the compressor	lb/sec
W_{bi}	Air-flow rate into chamber B	lb/sec
W_{bo}	Air-flow rate out of chamber B to the atmosphere	lb/sec
W_{ci}	Air-flow rate through the needle valve into chamber C	lb/sec
W_{co}	Air-flow rate out of chamber C	lb/sec
W_{cp}	Air-flow rate past the piston	lb/sec

SYMBOLS (Continued)

Symbol	Definition	Units
W_i	Air-flow rate into chamber A	lb/sec
W_o	Air-flow rate through exhaust nozzles in the manifold to the atmosphere	lb/sec
W_L	Air-flow rate through the duct to the manifold	lb/sec
W_V	Air-flow rate through the blow-off valve	lb/sec
x	Displacement of the surge sensor poppet ball from its seat	in.
y	Displacement of the blow-off valve cover or the opening of the needle valve	in.
θ	Referred temperature, $\frac{T_1}{518.4}$	
δ	Referred total pressure, $\frac{P_1}{14.7}$	

CONSTANTS

Symbol	Definition	Value
C	Flow coefficient for above critical flow	0.8
c_p	Specific heat at constant pressure	0.2417 Btu/lb^{o} - R
f_{31}, f_{32}, f_{3v}, f_1, f_{3p}	Flow parameters for above critical flow	$0.531 \frac{\sqrt{^{o}R}}{sec}$
g	Gravitational constant	386.4 in./sec^2
J	Mechanical equivalent of heat	778 ft-lb/Btu
$\frac{K_a}{\delta}$	Experimental constant for the air-flow rate relation for chamber A	$(0.343)10^{-3} \frac{lb/sec}{lb\text{-}in.^2}$
$\frac{K\delta}{\sqrt{\theta}}$	Experimental constant for the relation between P_2 and W_a	(4.08) (10^{-4}) sec^2/lb^2
R	Gas constant	639.6 in./^{o}R
π		3.1416

DIMENSIONS

Symbol	Definition	Value
A_{a1}	Area of the diaphragm between chamber A and chamber 2	7.06 in.^{2}
A_{a2}	Area of the diaphragm between chamber B and chamber 2	0.601 in.^{2}

SYMBOLS (Continued)

Symbol	Definition	Value
A_{c1}	Area of the diaphragm at the bottom of chamber C	40.72 in.^{2}
A_{c2}	Area of the cover of the blow-off valve	38.48 in.^{2}
A_D	Cross-sectional area of the duct	44.18 in.^{2}
A_i	Area of the inlet orifice in chamber B	0.00196 in.^{2}
A_o	Area of the outlet orifices in chamber B	0.003236 in.^{2}
A_p	Area of the poppet exposed to pressure from chamber C	0.0768 in.^{2}
A_x	Area for flow from chamber C to the atmosphere	0.694x in.^{2}
A_y	Area of the opening of the needle valve to chamber C	0.0387y in.^{2}
D_{c2}	Diameter of blow-off valve cover	7.0 in.
I	Moment of inertia of rotor	0.1805 ft-lb-sec^2
K_x	Spring constant in surge sensor	6 lb/in.
K_y	Spring constant in blow-off valve	32.8 lb/in.
m_x	Mass of moving part of surge sensor	$(3.675)(10^{-4})$ $\frac{\text{lb-sec}^2}{\text{in.}}$
m_y	Mass of moving part of blow-off valve	$(7.169)(10^{-3})$ $\frac{\text{lb-sec}^2}{\text{in.}}$
V_{AO}	Volume of chamber A with poppet valve closed	1.83 in.^{3}
V_{BO}	Volume of chamber B with poppet valve closed	0.196 in.^{3}
V_{CO}	Volume of chamber C with the blow-off valve closed	58.43 in.^{3}
V_M	Volume of the manifold	15321.15 in.^{3}

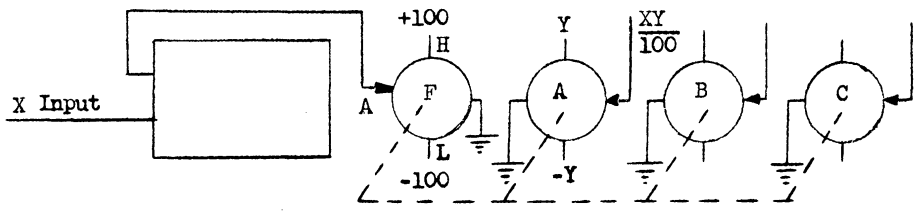

Servo Multiplier

3498-1-F

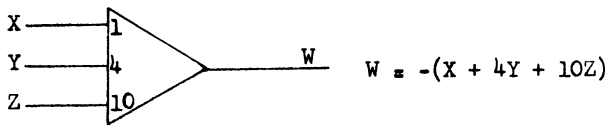

Summing Amplifier

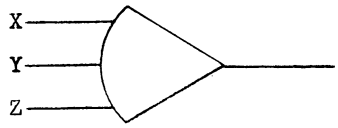

Amplifier with Feedback Removed

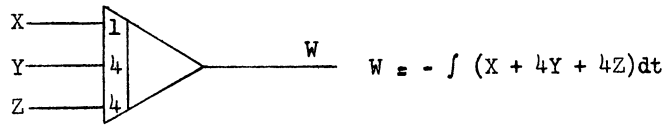

Integrator

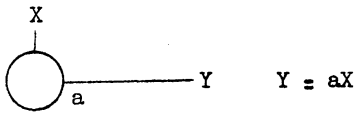

Scale-Factor Potentiometer

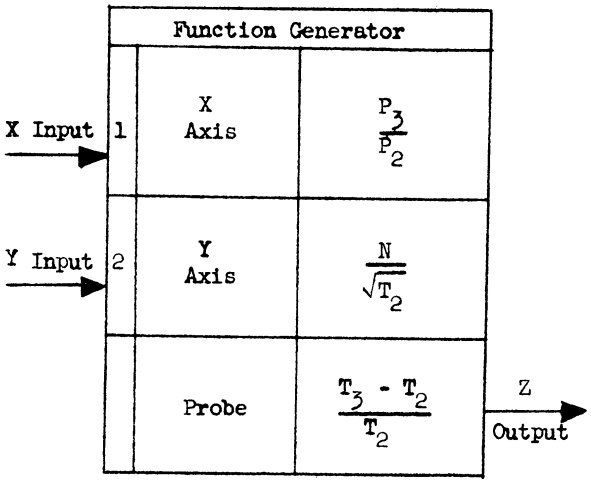

Dual-Input Function Generator Z = f(X, Y)

Analog Computer Investigation of a Boundary-Layer-Control System

ABSTRACT

A limited study using an analog computer was performed to investigate the stability of a pneumatic system consisting of a gas-turbine-driven compressor operating into a manifold from which air was escaping through a number of orifices. Simulation of linearized equations which describe the transient operation of the system for small departures from steady-state operating conditions was completed, and results of this simulation are presented. The results from this incomplete study show that the system has strong tendencies toward instability. A circuit for simulating the general nonlinear equations for the system is also presented. The linear and nonlinear simulations are compared. Methods of simulating a system consisting of a long manifold with one compressor at each end are discussed.

1
INTRODUCTION and CONCLUSIONS

1.1. INTRODUCTION

This is a final report on a study conducted by the Analog Computer Laboratory of Willow Run Laboratories of The University of Michigan for CAE (Continental Aviation and Engineering Corporation) under contract to the Air Force. The purpose of the study was to investigate, with an analog computer, the stability of a BLC (boundary-layer-control) system which was designed to change the flight characteristics of an aircraft by exhausting air through small holes distributed along the surface of the wing, thus disrupting the boundary layer of air at the wing's surface. The system consisted of a cylindrical manifold (90 feet long and 8.5 inches in diameter) which received air from two gas-turbine-driven compressors at each end and exhausted air through holes uniformly distributed along its length. Each of the compressors was fitted with an anti-surge control which opened a blow-off valve and thus increased the air flow from that particular compressor when its operation approached surge conditions.

The ultimate objective of the study was to simulate the entire system consisting of the manifold and four compressors, and to include the effects of pressure variations along the length of the manifold. The study was not, however, completed.

Initially, the analog computer was used to solve the linearized equations for one compressor, its anti-surge control, the duct, and the manifold. This preliminary investigation included the dynamics of the compressor and the inertial effects due to the mass of the moving elements of the controls. Since this resulted in a ninth-order system, a theoretical investigation would be quite difficult. This simulation was valid for small variations of variables from a steady-state operating point. The computer results are included in the report.

The digital program for obtaining steady-state points and the computer potentiometer settings is included in Appendix B.

The second phase of the study was to have been to simulate the nonlinear equations for the system.

Termination of the prime contract by the Air Force resulted in cancellation of this project; hence ultimate objectives of the contract were not fulfilled. A new contract was obtained from Continental Aviation and Engineering Corporation to write and publish this report.

1.2. CONCLUSIONS

Since the computer circuit used linearized equations which were valid for only very small changes of variables from a specific steady-state operating point, the results from the computer cannot give a complete description of the system's operation. Instead, the computer results merely indicate whether or not the system is stable at each operating point which was examined. When the system itself is in operation, an instability at some point causes the operation to shift to another point, which may be either more stable or less stable than the previous point. The nonlinear system could be regarded as a linear system in which the coefficients of the equations are continually changing and are functions of the instantaneous values of certain variables of the system.

The linearized equations are quite useful for a preliminary analog computer investigation of a system, since their mechanization on a computer requires a minimum of equipment; none of the less-accurate nonlinear computer components, such as multipliers and function generators, is used; and the linearized equations are less difficult to manipulate if it becomes desirable to verify analytically the validity of some unexpected result from the computer. Changing of the steady-state operating point for the computer mechanization requires a considerable amount of tedious hand computation to find the new steady-state values of variables and the potentiometer settings, although this part of the work may be performed quite rapidly on a digital computer.

A simulation of the general equations would be needed in order to completely explore the behavior of the system. This would permit the entire operating range of the system to be ex-

plored for regions of unsatisfactory operation, and would thus provide the system designer with a rather complete picture of its characteristics.

The following conclusions concerning operating characteristics of the system are based upon results obtained from simulating the linearized equations.

The simplified system, consisting of one compressor and anti-surge control operating into a manifold, is unstable when the blow-off valve is well open. This instability seems to be caused by similarities in magnitudes of time constants of the compressor, rotor, the manifold volume, and the control rate between the surge sensor and blow-off valve. If the manifold volume is increased the tendency toward instability is reduced. Also, the system becomes slightly more stable when the blow-off valve is nearly closed, probably because the time constant between the surge sensor and blow-off valve is increased under these conditions.

The blow-off valve itself has a tendency to oscillate at a frequency much higher than the natural system frequency. This tendency is strongest when the valve is nearly closed. This instability of the blow-off valve could be eliminated by installing a suitable viscous damping device, such as a dash pot, on the moving part of the blow-off valve.

Possibilities for unstable operation would be enormously increased if four compressors, each with an anti-surge control, were connected to a common manifold, because such an arrangement has many more feedback loops than the simplified system.

Although the simulation indicated that the system as described in this report is somewhat unstable, it is felt that the system instability may be eliminated by changing one of the three time constants mentioned earlier. Further computer investigation would probably show what changes should be made to make the system operation completely satisfactory.

2
THE BLC SYSTEM

2.1. DESCRIPTION OF THE BLC SYSTEM

Figure 1, which is reproduced from a drawing supplied by CAE, is a schematic diagram of the BLC system. The system consists of four gas-turbine-driven compressors which are forcing air into a single long cylindrical manifold. Air escapes from the manifold through a number of orifices distributed along its length. The duct from each compressor to the manifold contains a check valve to prevent air from flowing from the manifold to the compressor. Each compressor is equipped with an anti-surge system (not shown in Figure 1).

The system which was simulated is shown schematically in Figure 2. It consists of a single compressor and anti-surge control, working into a manifold having one-fourth of the volume of the manifold shown in Figure 1.

3498-1-F

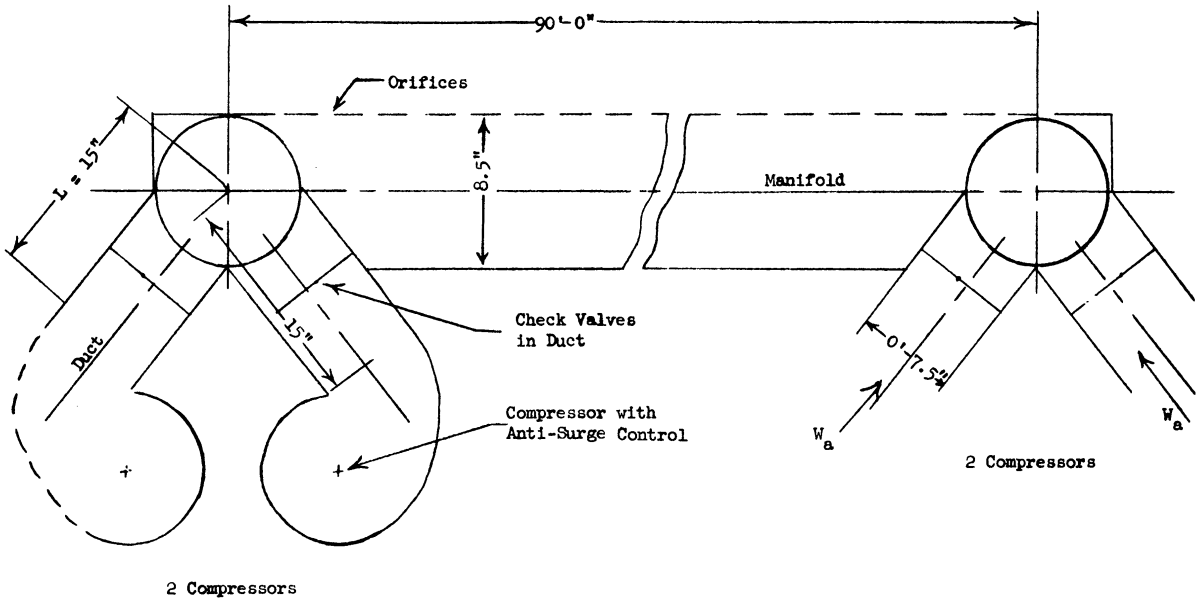

FIGURE 1. BLC SYSTEM

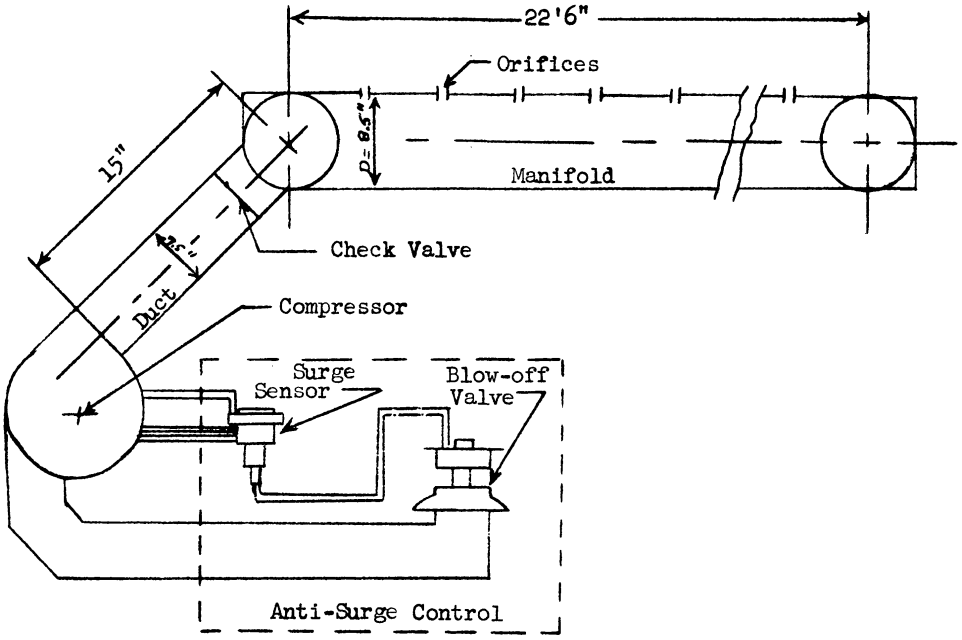

FIGURE 2. SINGLE-COMPRESSOR BLC SYSTEM

The anti-surge control consists of the surge sensor and the blow-off valve. The surge sensor is a pneumatic device which monitors the compressor air-flow rate and outlet pressure. When the compressor air flow decreases or compressor outlet pressure increases sufficiently to cause the compressor operation to approach surge conditions, the surge sensor causes the blow-off valve to open. This permits air from the compressor to escape through the blow-off valve, thus increasing the total air flow and removing the danger of surge.

A mechanical schematic diagram of the surge sensor and blow-off valve is shown in Figure 3. The difference between total pressure (P_1) and static pressure (P_2) at the compressor outlet is a function of air-flow rate from the compressor. This pressure difference applied across the diaphragm between chamber A and chamber 2 of the surge sensor causes a downward force to be exerted on the poppet valve at the bottom of the surge sensor. The pressure

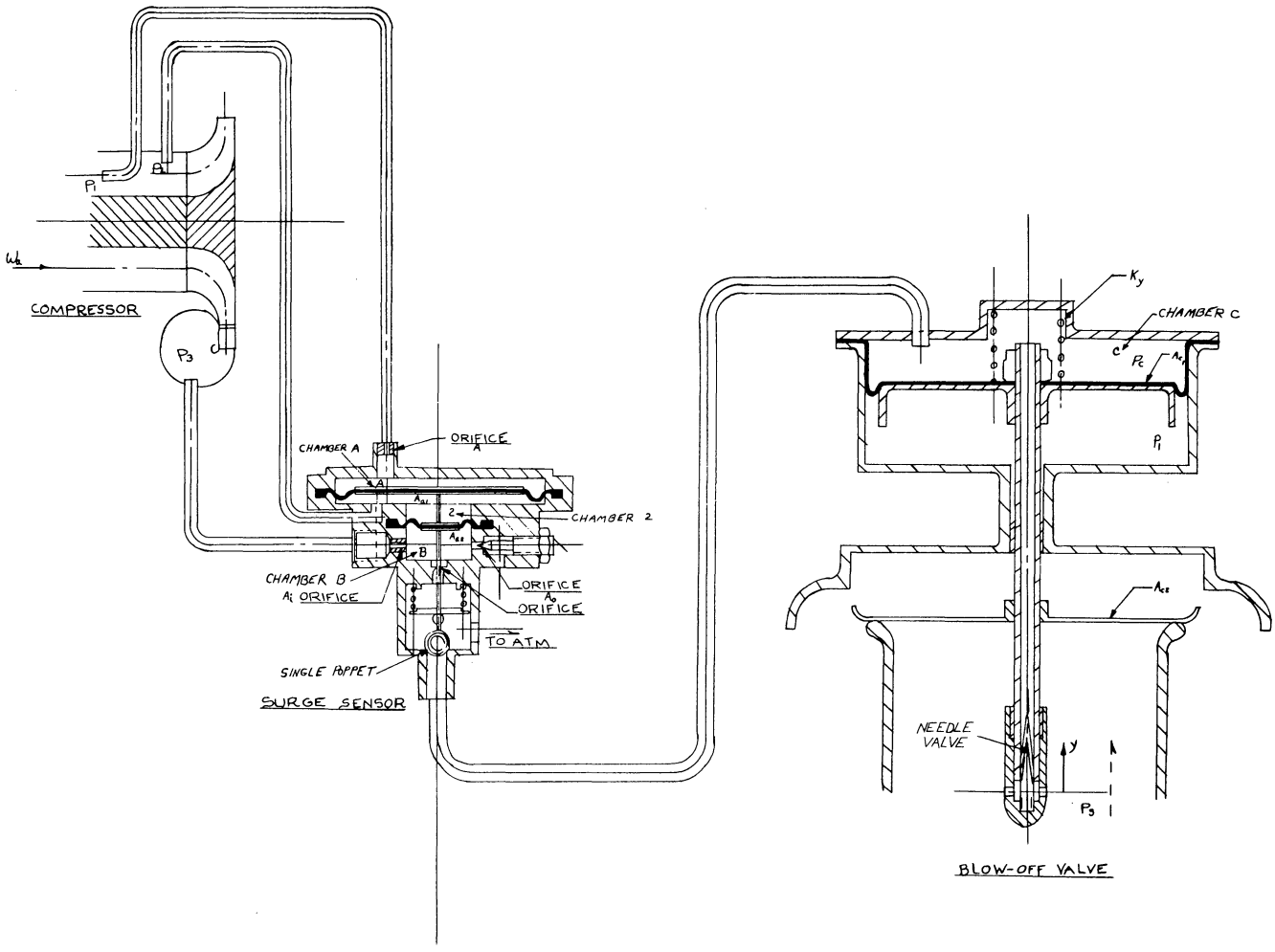

FIGURE 3. SCHEMATIC DIAGRAM OF ANTI-SURGE CONTROL

which is in chamber B is proportional to the compressor outlet pressure, and exerts an upward force on the valve. Whenever a stall condition is approached, the air flow from the compressor decreases, thereby causing a decrease in downward force on the poppet valve, and the compressor outlet pressure increases, thus causing an increase in upward force. This change of forces causes the valve to open, thus permitting air to escape from chamber C of the blow-off valve. The resulting drop in P_C permits the upward force on the valve due to P_3 to open the valve and permit air to escape. The upward motion of the blow-off valve also opens the needle valve at its base, and thus permits air to flow into chamber C. For a given opening of the surge-sensor poppet valve, the blow-off valve always assumes a steady-state position such that the air-flow rate into chamber C through the needle valve just equals that out through the poppet valve. When the poppet valve closes, the pressure in chamber C rises sufficiently to close the blow-off valve and needle valve.

Air passing through small orifices in chambers A and B of the surge sensor restricts the flow rates and thus improves the stability of the surge sensor by introducing damping effects.

2.2. DERIVATION OF EQUATIONS

Mathematical equations which describe the operation of the system are developed in this section.

For each major component of the system, first the general nonlinear equations are written, and then the linearized equations are derived. The linearized equations are specialized equations which describe the relationships between changes in system variables from their steady-state values. These equations are valid only for very small changes of variables, and are obtained by the process illustrated in this section.

2.2.1. COMPRESSOR. In functional notation, the compressor pressure ratio (P_3/P_1) may be expressed as a function of two variables, the corrected rotor speed $(N/\sqrt{\theta})$ and the corrected air-weight flow rate $(W_a\sqrt{\theta}/\delta)$:

$$\frac{P_3}{P_1} = f_1\left(\frac{N}{\sqrt{\theta}}, \frac{W_a\sqrt{\theta}}{\delta}\right). \qquad \text{(1NL)}$$

Similarly, the corrected temperature rise $\left(\frac{T_3 - T_1}{T_1}\right)$ may be expressed as another function of the same two variables:

$$\frac{T_3 - T_1}{T_1} = f_2\left(\frac{N}{\sqrt{\theta}}, \frac{W_a\sqrt{\theta}}{\delta}\right). \qquad \text{(2NL)}$$

Writing the total differential for $\frac{P_3}{P_1}$ in Equation 1NL, and for $\frac{T_3 - T_1}{T_1}$ in Equation 2NL gives

$$\Delta\frac{P_3}{P_1} = \left(\frac{\partial\frac{P_3}{P_1}}{\partial N}\bigg|_{W_a}\right)\Delta N + \left(\frac{\partial\frac{P_3}{P_1}}{\partial W_a}\bigg|_{N}\right)\Delta W_a . \qquad (1L)$$

$$\Delta\frac{T_3}{T_1} = \left(\frac{\partial\frac{T_3 - T_1}{T_1}}{\partial N}\bigg|_{W_a}\right)\Delta N + \left(\frac{\partial\frac{T_3 - T_1}{T_1}}{\partial W_a}\bigg|_{N}\right)\Delta W_a . \qquad (2L)$$

The operating characteristics of the centrifugal compressor which is used in the system were obtained from a "map" which had P_3/P_1 for its ordinate, $W_a\sqrt{\theta}/\delta$ for its abscissa, and contained lines of constant $N/\sqrt{\theta}$, and lines of constant efficiency. Using the Keenan and Kaye gas tables (Reference 1), the air temperature rise due to compression was computed from pressure ratio and compressor efficiency, as obtained from the map. The resulting data was then cross-plotted in a form which permitted graphical determination of the values of the partial derivatives in Equations 1L and 2L.

2.2.2. ROTOR DYNAMICS. The rate of kinetic energy storage in the compressor rotor is equal to the difference between power supplied by the turbine and power required by the compressor. In equation form

$$550\ Hp_T - Jc_pW_a(T_3 - T_1) = \left(\frac{2\pi}{60}\right)^2 I\dot{N}N, \qquad (3NL)$$

where Hp_T is the horsepower supplied by the turbine (assumed constant)

J is the mechanical equivalent of heat (778 ft-lb/Btu)

c_p is the specific heat of air

I is the moment of inertia of the combined compressor turbine rotor

N is the rotor speed (revolutions per minute)

The linearized form of Equation 3NL is

$$-Jc_p(T_3 - T_1)\,\Delta W_a - Jc_pW_a\Delta T_3 = \left(\frac{2\pi}{60}\right)^2 I\,(\dot{N}\Delta N + N\Delta\dot{N}).$$

Since for steady-state conditions $\dot{N} = 0$, the term $\dot{N}\Delta N$ may be eliminated, giving

$$\left(\frac{2\pi}{60}\right)^2 IN\Delta\dot{N} = -Jc_p(T_3 - T_1)\Delta W_a - Jc_pW_a\Delta T_3 . \qquad (3L)$$

2.2.3. SURGE SENSOR.[1] The anti-surge control uses the compressor air-weight flow and outlet pressure to control the position of the blow-off valve. The blow-off valve may be operated directly by compressor-outlet pressure, or it may be controlled by the surge sensor, which is controlled by compressor air-flow rate and compressor-outlet pressure.

Referring to Figure 3, the surge sensor contains chambers 2, A, and B, diaphragms A_{a1} and A_{a2}, orifices A, A_i, and A_o, a spring, and a single poppet valve. P_2 is the compressor-inlet static pressure. P_1 is the compressor-inlet total pressure. The pressure in chamber 2 of the surge sensor is P_2, the compressor-inlet static pressure, and thus is dependent on the rate of the air-weight flow through the compressor. If the air-weight flow decreases, the pressure in chamber 2 increases. Since diaphragm A_{a1} is larger than diaphragm A_{a2}, the force resulting from the pressure in chamber 2 is such that it tries to open the poppet valve. The inlet and outlet orifices of chamber B are adjusted in the cross-sectional area so that the pressure in chamber B is proportional to P_3, the compressor outlet pressure. The resulting force on diaphragm A_{a2} tends to open the poppet ball. Also, the force from the pressure in chamber C of the blow-off valve is pushing on the bottom of the poppet ball. There are two forces which tend to close the poppet valve. One force is proportional to the amount the spring is displaced from its equilibrium position. The other downward force results from the pressure in chamber A (the compressor-inlet total pressure, P_1) exerted on diaphragm A_{a1}. The rates of pressure change in chambers A and B are restricted by placing small orifices in the paths of air passing into and out of these chambers. This introduces damping and thus reduces the tendency of the surge sensor to oscillate.

When the poppet is open, air flows from chamber C in the blow-off valve through the poppet to the atmosphere by way of an opening in the side of the surge sensor.

If the probes which sense static and total pressures at the compressor inlet are properly adjusted,

$$\frac{P_1 - P_2}{P_1} = K\left(\frac{W_a\sqrt{\theta}}{\delta}\right)^2 . \qquad (4NL)$$

Assuming laminar flow through orifice A, $W_{ai} = K_a(P_1 - P_A)$. Combining this with the general gas-law equation for chamber A gives

$$\frac{P_A V_A}{RT_A} = \int W_{ai}\,dt = \int K_a(P_1 - P_A)\,dt. \qquad (5NL)$$

[1] Most of the equations and parameters which are used in this section were obtained from a Cosmodyne Corporation report (Reference 2).

For the volume of chamber A,

$$V_A = V_{AO} - A_{a1}x, \tag{6NL}$$

where V_{AO} is the volume of chamber A with the poppet valve closed, and x is the displacement of the poppet ball off its seat.

The flow from the compressor outlet into chamber B through orifice A_i is given by the equation

$$W_{bi} = \frac{Cf_{31}A_iP_3}{\sqrt{T_B}}, \tag{7NL}$$

where f_{31} is the flow parameter

C is the flow coefficient

A_i is the cross-sectional area of orifice A_i

T_B is the temperature of the air in chamber B

The flow from chamber B to the atmosphere is through two orifices labeled A_o. The combined cross-sectional area of these two orifices is A_o, and the flow is given by

$$W_{bo} = \frac{Cf_{32}A_oP_B}{\sqrt{T_B}}. \tag{8NL}$$

The volume of chamber B is

$$V_B = V_{BO} + A_{a2}x, \tag{9NL}$$

where V_{BO} is the volume of chamber B with the poppet valve closed, and x is the same as for Equation 6NL. The gas-law equation for chamber B is

$$\frac{P_BV_B}{RT_B} = \int (W_{bi} - W_{bo})\,dt. \tag{10NL}$$

The force equation for the surge sensor, for $x > 0$, is written by setting the sum of the upward forces equal to the reaction force due to acceleration:

$$-F_o + A_p(P_C - P_1) + A_{a2}P_B + (A_{a1} - A_{a2})P_2 - A_{a1}P_A - K_xx = m_x\ddot{x}, \tag{11NL}$$

where F_o is the spring force when x is zero

A_p is effective area of the poppet valve

K_x is the spring constant

m_x is the mass of the moving part of the surge sensor

Equations 4NL through 11NL may be linearized by writing the total differentials as was done for the compressor. These linearized equations are listed below.

$$-\frac{\Delta P_2}{P_1} = \frac{2KW_a}{\delta^2}\theta\Delta W_a . \tag{4L}$$

$$\frac{V_A\Delta P_A}{RT_A} + \frac{P_A\Delta V_A}{RT_A} = -K_a\int\Delta P_A\,dt . \tag{5L}$$

$$\Delta V_A = -A_{a1}\Delta x . \tag{6L}$$

$$\Delta W_{bi} = \frac{Cf_{31}A_i}{\sqrt{T_B}}\Delta P_3 + \frac{CA_iP_3}{\sqrt{T_B}}\Delta f_{31} . \tag{7L}$$

$$\Delta W_{bo} = \frac{Cf_{32}A_o}{\sqrt{T_B}}\Delta P_B + \frac{CA_oP_B}{\sqrt{T_B}}\Delta f_{32} . \tag{8L}$$

$$\Delta V_B = A_{a2}\Delta x . \tag{9L}$$

$$\frac{V_B\Delta P_B}{RT_B} + \frac{P_B\Delta V_B}{RT_B} = \int(\Delta W_{bi} - \Delta W_{bo})\,dt . \tag{10L}$$

$$A_p\Delta P_C + A_{a2}\Delta P_B + (A_{a1} - A_{a2})\Delta P_2 - A_{a1}\Delta P_A - K_x\Delta x = m_x\Delta\ddot{x} . \tag{11L}$$

2.2.4. BLOW-OFF VALVE. Functional components of the blow-off valve include a spring, chamber C, diaphragm A_{c1}, a needle valve which allows air at P_3 to flow into chamber C, and a large valve of diameter D_{c2} and area A_{c2} which can release compressor-outlet air to the atmosphere.

The downward force exerted by the pressure in chamber C acting on diaphragm A_{c1} tends to close the blow-off valve. The spring applies a downward force which is directly proportional to its displacement from its equilibrium position. Thus, the spring force also tends to close the blow-off valve. The upward forces on the valve are caused by P_3, the compressor-outlet pressure, acting on the bottom of A_{c2}, and P_1 acting on the bottom of diaphragm A_{c1}.

If the pressure in chamber C is reduced sufficiently due to air flow out of this chamber through the poppet valve in the surge sensor, the forces holding the blow-off valve closed will be decreased, and the valve will open. Excess compressor air flow is then bled through the valve, permitting the compressor air-flow rate to increase, and preventing the compressor's

operating point from crossing the surge line on the compressor map. The opening of the blow-off valve also opens a needle valve which permits air from the compressor outlet (at pressure P_3) to flow into chamber C. This permits the air pressure in C to build up and the blow-off valve to close whenever the poppet valve in the surge sensor closes.

With the poppet valve and the blow-off valve closed, the three factors which determine when the anti-surge control begins to operate are the forces from the springs, the calibration of the sensing probes, and the adjustment of orifice A_o in chamber B.

The bleed air-weight flow to the atmosphere through the blow-off valve is given by the equation

$$W_v = \frac{CP_3 f_{3v} \pi D_{c2} y}{\sqrt{T_3}}, \qquad (12NL)$$

where y is the displacement of the large valve from its seat

$\pi D_{c2} y$ is the area of the opening of the large valve

f_{3v} is the flow parameter

If the flow through the needle valve from the compressor to chamber C is assumed to be incompressible, then the flow rate is given by

$$W_{ci} = Cy \frac{dA_y}{dy} \sqrt{\frac{2gP_3}{RT_3}(P_3 - P_C)}, \qquad (13NL)$$

where $A_y = y \frac{dA_y}{dy}$ is the area of the needle valve opening, as a function of y.

The air flow out of chamber C enters the surge sensor through an area A_x in the poppet valve. The flow rate is given by

$$W_{co} = \frac{Cf_{33} P_C A_x}{\sqrt{T_C}}, \qquad (14NL)$$

where f_{33} is the flow parameter. An approximation of the area is

$$A_x = 0.694x. \qquad (15NL)$$

The volume of chamber C is given by

$$V_C = V_{CO} - A_{c1} y, \qquad (16NL)$$

where V_{CO} is the volume of chamber C with the blow-off valve closed.

Applying the gas-law equation to the air in chamber C gives

$$\frac{P_C V_C}{RT_C} = \int (W_{ci} - W_{co})\, dt, \tag{17NL}$$

where W_{ci} is the rate of air flow into the chamber through the needle valve

W_{co} is the rate of air flow out through the poppet valve in the surge sensor

The expression for a force balance in the blow-off valve for $y > 0$ is

$$-H_o + (P_3 - P_1)A_{c2} - (P_C - P_1)A_{c1} - K_y y = m_y \ddot{y}, \tag{18NL}$$

where H_o is the spring force when y is zero

K_y is the spring constant

m_y is the mass of the moving part of the blow-off valve

If a piston is used instead of diaphragm A_{c1}, three changes in the equations take place. First, mass m_y is increased; second, there is leakage from chamber C to the atmosphere around the piston; and third the force-balance equation must include a term to represent the friction between the piston and the cylinder wall. (See the next two sections for Equations 19NL through 22NL.)

The leakage air-flow rate for the piston is given by

$$W_{cp} = \frac{C f_{3p} P_C A_L}{\sqrt{T_C}}, \tag{23NL}$$

where f_{3p} is the flow parameter

A_L is the effective area of the leakage path

The gas-law equation for chamber C is modified by adding the leakage term, W_{cp}:

$$\frac{P_C V_C}{RT_C} = \int (W_{ci} - W_{co} - W_{cp})\, dt. \tag{24NL}$$

The friction force between the piston and cylinder wall is a constant which changes sign when the piston reverses its direction of motion, as shown in Figure 4.

This coulomb friction force of magnitude B may be represented mathematically by the expression $\frac{\dot{y}}{|\dot{y}|}B$, and adding this force to the force-balance equation for the blow-off valve gives

$$-H_o + (P_3 - P_1)A_{c2} - (P_C - P_1)A_{c1} - K_y y = m_y \ddot{y} + \frac{\dot{y}}{|\dot{y}|}B. \tag{25NL}$$

3498-1-F

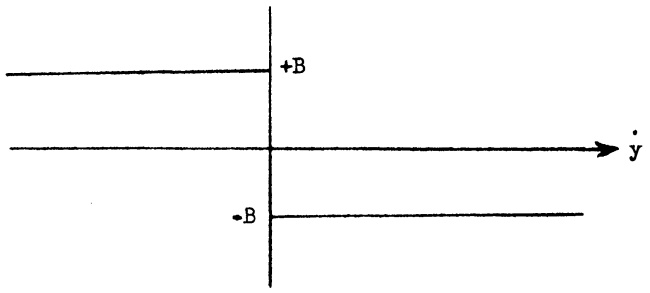

FIGURE 4. COULOMB FRICTION

Equations 12NL through 18NL and Equations 23NL and 24NL can be linearized to give the following equations.

$$\Delta W_V = \left(\frac{Cf_{3v}\pi D_{c2}}{\sqrt{T_3}}\right)(y\Delta P_3 + P_3\Delta y). \tag{12L}$$

$$\Delta W_{ci} = C\frac{dA_y}{dy}\sqrt{\frac{2g}{RT_3}}\left[\frac{y(2P_3 - P_C)\Delta P_3}{2\sqrt{P_3^2 - P_3P_C}} - \frac{yP_3\Delta P_C}{2\sqrt{P_3^2 - P_3P_C}} + \left(\sqrt{P_3^2 - P_3P_C}\right)\Delta y\right]. \tag{13L}$$

$$\Delta W_{co} = \frac{Cf_{33}}{\sqrt{T_C}}(A_x\Delta P_C + P_C\Delta A_x) + \frac{CP_CA_x}{\sqrt{T_C}}\Delta f_{33}. \tag{14L}$$

$$\Delta A_x = 0.694\Delta x. \tag{15L}$$

$$\Delta V_C = -A_{c1}\Delta y. \tag{16L}$$

$$\frac{\Delta P_C V_C}{RT_C} + \frac{P_C}{RT_C}\Delta V_C = \int(\Delta W_{ci} - \Delta W_{co})\,dt. \tag{17L}$$

$$A_{c2}\Delta P_3 - A_{c1}\Delta P_C - K_y\Delta y = m_y\Delta\ddot{y}. \tag{18L}$$

$$\Delta W_{cp} = \frac{Cf_{3p}A_L\Delta P_C}{\sqrt{T_C}}. \tag{23L}$$

$$\frac{\Delta P_C V_C}{RT_C} + \frac{P_C\Delta V_C}{RT_C} = \int(\Delta W_{ci} - \Delta W_{co} - \Delta W_{cp}). \tag{24L}$$

2.2.5. DUCT. Air from the compressor outlet has four possible exits. Most of the air flow is through the duct into the manifold and through the blow-off valve, but some also flows into chamber B of the surge sensor and chamber C of the blow-off valve. Thus, the total air-flow rate (W_a) is the sum of these four separate air-flow rates. In equation form,

$$W_a = W_L + W_V + W_{bi} + W_{ci}. \tag{19NL}$$

Since the pressure drop across the duct is quite small, the incompressible-flow equation may be used:

$$W_L = CA_3 \sqrt{\frac{2g}{RT_3}} \sqrt{P_3(P_3 - P_M)}, \tag{20NL}$$

and

$$W_L = 0 \text{ for } (P_3 - P_M) < 0, \quad \text{(check valve closed)}$$

where A_3 is the cross-sectional area of the duct

P_M is the manifold pressure

Equations 19NL and 20NL may be linearized to give

$$\Delta W_a = \Delta W_L + \Delta W_V + \Delta W_{bi} + \Delta W_{ci}. \tag{19L}$$

$$\Delta W_L = \frac{CA_3\sqrt{\frac{2g}{RT_3}}}{2\sqrt{P_3(P_3 - P_M)}} \left[(2P_3 - P_M)\Delta P_3 - P_3 \Delta P_M\right]. \tag{20L}$$

2.2.6. MANIFOLD. The manifold pressure, P_M, is always very much greater than atmospheric pressure, P_1, so the flow parameter used in the equation which describes air flow from the manifold through the exhaust orifices is a constant. The flow equation is

$$W_o = \frac{f_1 CA_M P_M}{\sqrt{T_M}}, \tag{21NL}$$

where f_1 is the flow parameter

A_M is the combined area of all the exhaust nozzles

The gas-law equation for the manifold is

$$\frac{P_M V_M}{RT_M} = \int (W_L - W_o)\, dt. \tag{22NL}$$

The volume of the manifold for the case of one compressor was taken to be one-fourth the volume of the manifold shown in Figure 1.

The manifold equations can be linearized to give

$$\Delta W_o = \frac{f_1 C A_M}{\sqrt{T_M}} \Delta P_M, \tag{21L}$$

and

$$\frac{\Delta P_M V_M}{R T_M} = \int (\Delta W_L - \Delta W_o)\, dt. \tag{22L}$$

3
ANALOG COMPUTER MECHANIZATION of LINEARIZED EQUATIONS

Linearized Equations 1L through 22L, Section 2.2.1 through 2.2.6, are, in principle, the equations solved by the analog computer to obtain a linearized simulation of the system. The actual equations which were mechanized are listed in this section. The assumptions which are applicable to each equation are also stated.

The constant coefficients are designated as α's with subscripts; their definitions are given in Section 3.2.

3.1. EQUATIONS MECHANIZED FOR COMPUTER

The number or numbers in parentheses to the left of each equation indicate which equations, from Sections 2.1 through 2.6, are used.

Compressor and Rotor Dynamics

(1L) $$\Delta P_3 = \alpha_1 \Delta N + \alpha_2 \Delta W_a, \tag{1C}$$

where $\alpha_1 > 0$ and $\alpha_2 > 0$.

(2L, 3L) $$\dot{\Delta N} = -\alpha_3 \Delta W_a - \alpha_4 \Delta N. \tag{2C}$$

Surge Sensor

In chamber A, assume $T_A = T_1$.

(5L, 6L) $$\dot{\Delta P}_A = \alpha_5 \dot{\Delta x} - \alpha_6 \Delta P_A. \tag{3C}$$

In chamber B, assume that $T_B = T_3$ and that f_{31} and f_{32} are constants (choke flow through orifices A_i and A_o).

(7L, 8L, 9L, 10L) $$\dot{\Delta P}_B = \alpha_7 \Delta P_3 - \alpha_8 \Delta P_B - \alpha_9 \dot{\Delta x}. \quad (4C)$$

The force-balance equation for the surge sensor is

(11L, 4L) $$m_x \ddot{\Delta x} = A_p \Delta P_C + A_{a2} \Delta P_B - \alpha_{10} \Delta W_a - A_{a1} \Delta P_A - K_x \Delta x. \quad (5C)$$

Blow-Off Value

In chamber C, assume that $T_C = T_3$ and that f_{33} is a constant.

(13L, 14L, 15L, 16L, 17L)

$$\dot{\Delta P}_C = \alpha_{11} \Delta P_3 + \alpha_{12} \Delta y - \alpha_{13} \Delta P_C - \alpha_{14} \Delta x + \alpha_{15} \dot{\Delta y}. \quad (6C)$$

The force-balance equation is

(18L) $$m_y \ddot{\Delta y} = A_{c2} \Delta P_3 - A_{c1} \Delta P_C - K_y \Delta y. \quad (7C)$$

Duct and Manifold

Assume $T_M = T_3$.

(7L, 12L, 13L, 19L, 20L)

$$\Delta W_a = \alpha_{16} \Delta P_3 - \alpha_{17} \Delta P_C + \alpha_{18} \Delta y - \alpha_{19} \Delta P_M. \quad (8C)$$

(20L, 21L, 22L) $$\dot{\Delta P}_M = \alpha_{20} \Delta P_3 - \alpha_{21} \Delta P_M. \quad (9C)$$

3.2. DEFINITIONS OF COEFFICIENTS

Each α corresponds to a potentiometer in the computer mechanization, and the value of each α at a steady-state operating point determines the setting of the corresponding potentiometer.

$$\alpha_1 = P_1\left(\frac{\partial\frac{P_3}{P_1}}{\partial N}\bigg|_{W_a}\right)$$

$$\alpha_2 = P_1\left(\frac{\partial\frac{P_3}{P_1}}{\partial W_a}\bigg|_{N}\right)$$

$$\alpha_3 = \frac{Jc_p}{\left(\frac{2\pi}{60}\right)^2 IN}\left[T_3 - T_1 + T_1 W_a\left(\frac{\partial\frac{T_3 - T_1}{T_1}}{\partial W_a}\bigg|_{N}\right)\right]$$

$$\alpha_4 = \frac{Jc_p W_a T_1}{\left(\frac{2\pi}{60}\right)^2 IN}\left(\frac{\partial\frac{T_3 - T_1}{T_1}}{\partial N}\bigg|_{W_a}\right)$$

$$\alpha_5 = \frac{P_A A_{a1}}{V_A}$$

$$\alpha_6 = \frac{K_a R T_1}{V_A}$$

$$\alpha_7 = \frac{Cf_{31} A_i R\sqrt{T_3}}{V_B}$$

$$\alpha_8 = \frac{Cf_{32} A_o R\sqrt{T_3}}{V_B}$$

$$\alpha_9 = \frac{A_{a2} P_B}{V_B}$$

$$\alpha_{10} = \frac{2KP_1 W_a \theta}{\delta^2}(A_{a1} - A_{a2})$$

$$\alpha_{11} = \frac{Cy\frac{dA_y}{dy}\sqrt{2gRT_3}(2P_3 - P_C)}{2V_C\sqrt{P_3(P_3 - P_C)}}$$

$$\alpha_{12} = \frac{C\frac{dA_y}{dy}\sqrt{2gRT_3P_3(P_3 - P_C)}}{V_C}$$

$$\alpha_{13} = \frac{Cf_{33}A_xR\sqrt{T_3}}{V_C} + \frac{Cy\frac{dA_y}{dy}P_3\sqrt{2gRT_3}}{2V_C\sqrt{P_3(P_3 - P_C)}}$$

$$\alpha_{14} = \frac{Cf_{33}P_C}{V_C}R\sqrt{T_3}\,(0.694)$$

$$\alpha_{15} = \frac{P_CA_{c1}}{V_C}$$

$$\alpha_{16} = \frac{Cf_{31}A_i}{\sqrt{T_3}} + \frac{C\pi D_{c2}f_{3v}y}{\sqrt{T_3}} + \frac{Cy\frac{dA_y}{dy}\sqrt{\frac{2g}{RT_3}}}{2\sqrt{P_3(P_3 - P_C)}}(2P_3 - P_C)$$

$$+ \frac{CA_3\sqrt{\frac{2g}{RT_3}}(2P_3 - P_M)}{2\sqrt{P_3(P_3 - P_M)}}$$

$$\alpha_{17} = \frac{Cy\frac{dA_y}{dy}\sqrt{\frac{2g}{RT_3}}}{2\sqrt{P_3(P_3 - P_C)}}P_3$$

$$\alpha_{18} = \frac{C\pi D_{c2}f_{3v}P_3}{\sqrt{T_3}} + C\frac{dA_y}{dy}\sqrt{\frac{2g}{RT_3}P_3(P_3 - P_C)}$$

$$\alpha_{19} = \frac{CA_3\sqrt{\frac{2g}{RT_3}}}{2\sqrt{P_3(P_3 - P_M)}}P_3$$

$$\alpha_{20} = \frac{CA_3\sqrt{2gRT_3}}{2V_M\sqrt{P_3(P_3 - P_M)}}(2P_3 - P_M)$$

$$\alpha_{21} = \frac{CA_3P_3\sqrt{2gRT_3}}{2V_M\sqrt{P_3(P_3 - P_M)}} + \frac{R\sqrt{T_3}f_1CA_M}{V_M}$$

3.3. COMPUTER MECHANIZATION

Figure 5 is a block diagram of the linear simulation. Each block represents a separate component of the system, as indicated, and contains equations which show the mathematical relationships between its input and output variables. The information flow shows exchange of ΔP_3 and ΔW_a information between the compressor and the duct. The surge sensor receives ΔP_3 from the compressor, ΔW_a from the duct, and ΔP_C from the blow-off valve. It sends Δx information to the latter. The blow-off valve also receives ΔP_3 information and transmits ΔP_C and Δy to the duct and manifold block.

An unscaled diagram of the computer mechanization which solves the equations in each block is shown in Figure 6. The symbols representing analog computer components are defined at the front of this report. The computer diagram is labeled to correspond to the blocks. One equation is not mechanized as specified; it is Equation 8C in the duct and manifold. The first term of this equation is $\alpha_{16}\Delta P_3$, which is obtained by substituting Equation 1C from the compressor and rotor dynamics. Therefore, ΔN is fed to a potentiometer set at $(\alpha_{16})(\alpha_1)$, and, likewise, ΔW_a is fed to a potentiometer set at $(\alpha_2)(\alpha_{16})$.

The mechanization uses 9 integrators, 9 summing amplifiers, and 31 coefficient potentiometers. Amplifier A and integrator B with potentiometers α_1, $-\alpha_2$, α_3, and α_4 solve equations which describe the compressor and rotor dynamics. Note that one potentiometer multiplies by $-\alpha_2$ instead of α_2 because α_2 is physically a negative number in this case, and potentiometers can have only positive settings.

Integrators C and D solve the gas-law equations for chambers B and A in the surge sensor, while integrators E and F with amplifier G solve the dynamics of the moving parts of the surge sensor.

The blow-off valve equations are solved in the lower right of the diagram by integrators H, I, and J, and amplifier K.

Integrator L's output is the pressure in the manifold, and amplifier M's output is the rate of air-weight flow from the compressor.

Because of the high response speed of certain parts of the system, it was impractical to use a "real-time" computer simulation (one in which computer operating time exactly corre-

3498-1-F

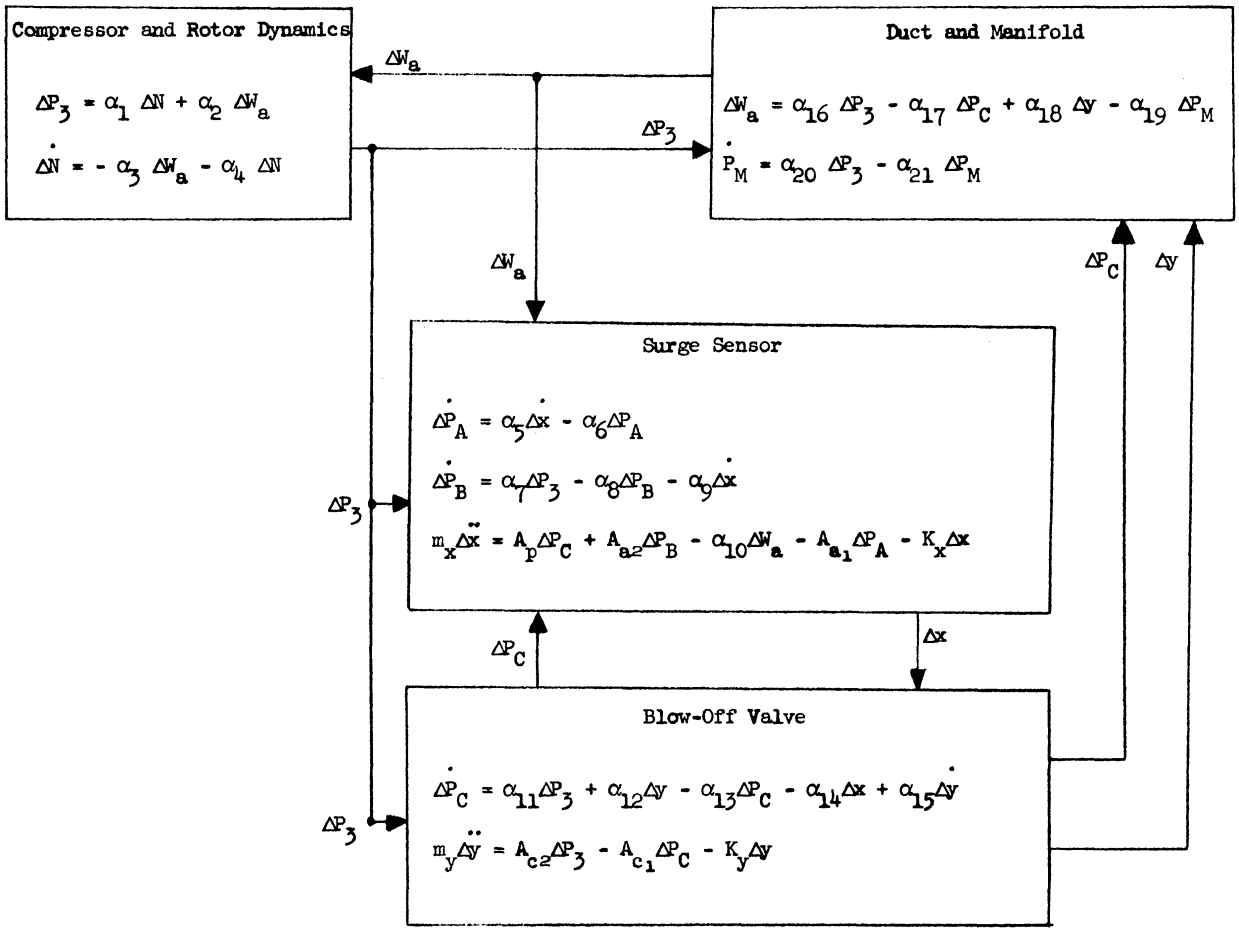

FIGURE 5. LINEAR SIMULATION

sponds to the operating time for the system). The solution on the computer was slowed down by a factor of 100, thus making 100 seconds of computer time correspond to 1 second of operating time for the system.

This time-scale change affects the scaling of the problem by multiplying the gain of the integrators in the computer mechanization by the ratio of computer time to problem time (in this case, 100). Therefore, if the quantity $\Delta \dot{P}_M$ is used as an input to an integrator with a nominal gain of unity (1 megohm input resistor and a 1 mfd feedback capacitor), the output of the integrator is 100 ΔP_M.

The dotted lines immediately below integrator I in the computer diagram, Figure 6, show the mechanization of the coulomb friction of the piston, which was added to chamber C in the blow-off valve. The term $\frac{\dot{y}}{|\dot{y}|} B$ of Equation 25NL is generated by a high-gain amplifier with its output limited to ±100 volts, and a potentiometer which converts this output to a voltage corresponding to the friction force B which, in turn, is added to the other forces entering integrator I. The term in Equation 23L which represents leakage air-flow rate for the piston has a

3498-1-F

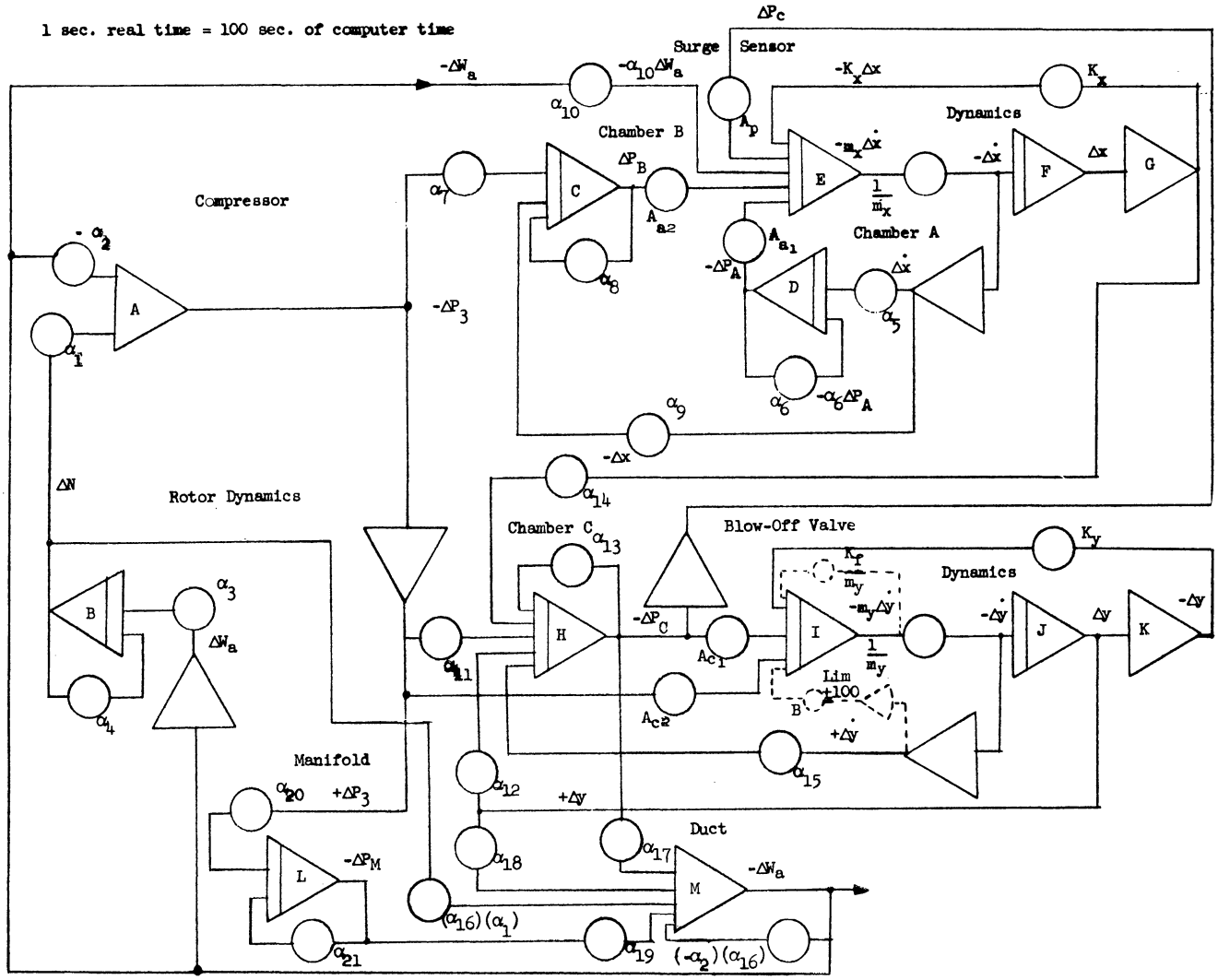

FIGURE 6. COMPUTER MECHANIZATION OF THE LINEAR EQUATIONS

coefficient of $\frac{Cf_{3p}A_L}{\sqrt{T_3}}$, which must be added to α_{13}. The setting of potentiometer α_{13} in the feedback loop of integrator H will contain this added quantity when the piston is added. Several runs on the computer were made with the piston and are presented in Section 4.

The computer diagram also shows the potentiometer which is added to simulate the operation of a dash pot placed on the blow-off valve. This potentiometer, which is in the feedback loop of integrator I, is set to $\frac{K_f}{m_y}$ and produces at its output the friction force due to the dash pot.

4
COMPUTER DATA

The data presented in this section was recorded from the computer mechanization of the linear equations. Transient data was obtained in terms of the departures of variables from their steady-state values. Three different cases of steady-state operating conditions were explored. The steady-state solutions for each case were found by hand computation, and parameters from the steady-state solutions were used to compute the potentiometer settings.

The first case was for both valves in the surge sensor and blow-off valve just closed ($y = 0$, $x = 0$). In the second case, the steady-state condition was for $y = 0.4$ inch, $x = 0.01043$ inch. For the third case, the steady-state condition was for $y = 0.8$ inch, $x = 0.01193$ inch.

For all three cases, the same operating point on the compressor map was used; therefore only one set of values for the compressor partial derivatives was required. The steady-state operating point was changed from one case to the next by changing the total area of the exhaust orifices, A_M, in the manifold, and thus changing W_o, and consequently W_L. The manifold volume remained constant at one-fourth the volume of the manifold shown in Figure 1. The adjustable valve (A_o) in chamber B was also changed.

Table I shows the steady-state values of the parameters used for each of the three cases, and Table II shows the values of the coefficients of the linearized equations for all three cases.

4.1. CASE 1 WITHOUT DAMPING

A computer run made for case 1 (valves just closed) is shown in Figure 7. This figure shows eight variables of the system plotted as functions of time by a Sanborn recorder. The time marks along the lower edge of the record mark off one-second intervals in computer time, which are equivalent to 0.01-second intervals for the problem. A time scale, in terms of problem time, is also shown along the lower edge of the figure. The eight variables which are plotted as functions of time are, from top to bottom on the figure, ΔW_a, Δx, Δy, ΔN, ΔP_C, ΔP_M, ΔP_B, and ΔP_3. The Δ's represent incremental departures from steady-state values of the variables.

The scaling shown for the ranges of Δ's in the figure is such that the curves show the response of the linearized equations to a step decrease of W_L of 1 pound per second at time $t = 0$. Since the equations are linear, all of the scales at the left side of the figure could be reduced by a factor of $1/K$, and the curves would be correct for a step decrease of $1/K$ pound per second of W_L at time $t = 0$.

Thus, by using the scales shown, the curves may be interpreted in terms of the change of each variable per pound per second step decrease in W_L. Since the linearized equations are

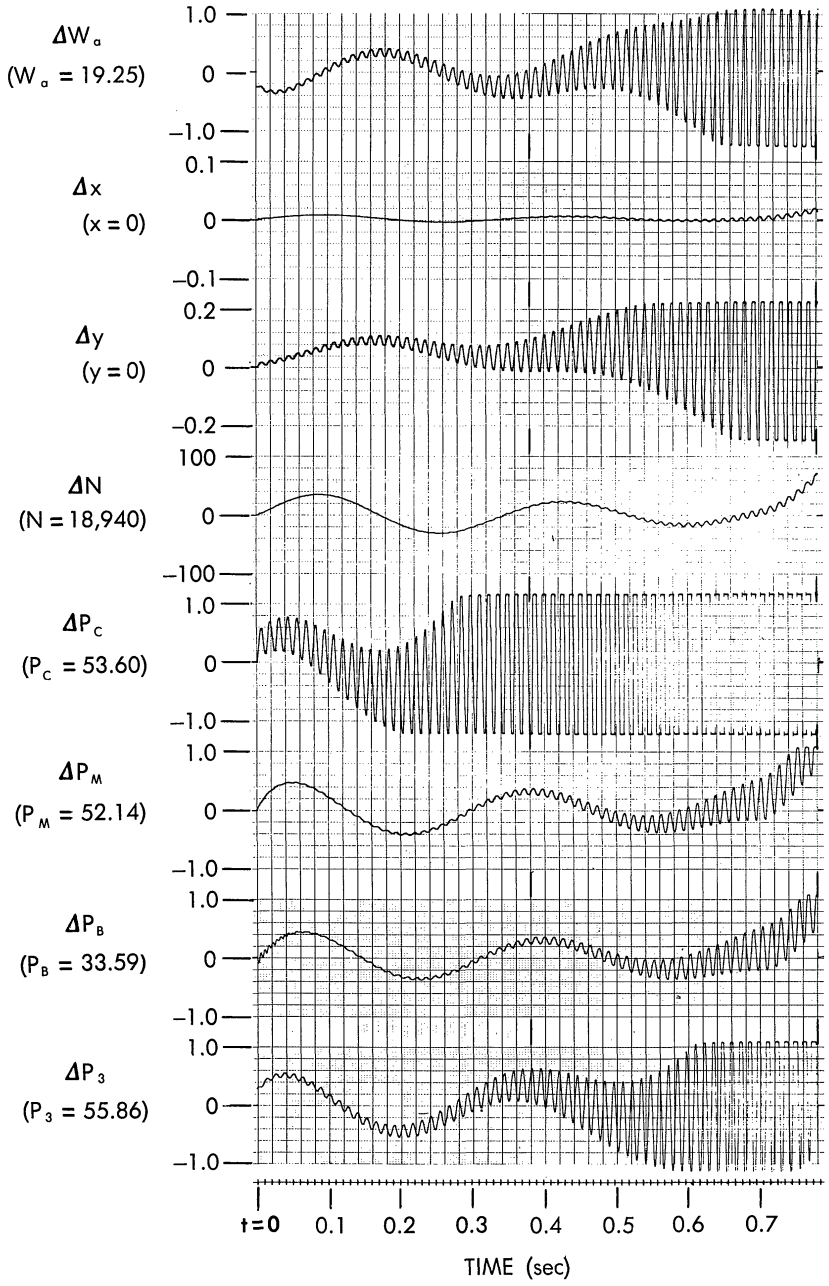

FIGURE 7. CASE 1 WITHOUT DAMPING

TABLE I. STEADY-STATE VALUES FOR PARAMETERS

$W_a = 19.25$, $P_3 = 55.86$, $T_3 = 846.7$, $P_2 = 12.48$, $W_{bi} = 1.589 \times 10^{-3}$, $\frac{N}{\sqrt{\theta}} = 18,940$, and $P_A = P_1 = 14.7$

	Case 1	Case 2	Case 3
x	0	0.01042	0.02224
y	0	0.4	0.8
P_B	33.59	33.74	33.79
P_C	53.60	53.27	52.95
P_M	52.14	54.40	55.62
W_{ci}	0	0.005627	0.01193
W_L	19.25	12.08	4.90
W_V	0	7.173	14.346
A_o	3.241×10^{-3}	3.226×10^{-3}	3.221×10^{-3}
A_M	25.29	15.21	6.035

applicable to the nonlinear system for only very small changes of the variables, the curves should not be interpreted in terms of absolute magnitudes of the Δ's, but instead in terms of relative magnitudes.

The steady-state value of each variable is indicated near the zero mark for the Δ scale.

For case 1, both valves were closed, so in the actual system a negative value of Δx or Δy would be impossible. These restrictions on Δx and Δy could have been introduced into the computer circuit by the use of diode-limiting circuits, but it was considered preferable to first examine the operation with no nonlinearities in the equations. If the Δ's were extremely small and the valves were just barely open, the curves for case 1 would be applicable and negative values of Δx and Δy would be permissible.

The step decrease in W_L may be interpreted as an equivalent step increase in the manifold pressure (caused, perhaps, by a sudden increase of air flow from one of the other compressors in a four-compressor BLC system). It does not cause a step on the ΔP_M curve in Figure 7, because the recorder stylus for this curve was connected to a point in the analog circuit at which the step would not appear. Instead, the ΔP_M curve shows the variations of P_M about the value which resulted from adding the step.

TABLE II. COEFFICIENT VALUES FOR PARAMETERS

Coefficients	Case 1	Case 2	Case 3
	Compressor and Rotor		
α_1	0.0062	0.0062	0.0062
α_2	-1.176	-1.176	-1.176
α_3	1841.4	1841.4	1841.4
α_4	2.699	2.699	2.699
	Surge Sensor		
α_5	56.71	58.97	62.15
α_6	62.34	64.82	68.31
α_7	78.62	76.28	73.73
α_8	130.7	126.3	121.9
α_9	103.0	100.4	97.17
α_{10}	1.491	1.491	1.491
	Blow-Off Valve		
α_{11}	0	14.62	45.16
α_{12}	121.8	180.7	312.3
α_{13}	0	15.31	47.64
α_{14}	5034	6935	11235.2
α_{15}	37.35	51.46	83.38
	Duct and Manifold		
α_{16}	2.761	4.368	10.487
α_{17}	0	1.086×10^{-3}	2.0×10^{-3}
α_{18}	17.94	17.94	17.95
α_{19}	2.587	4.128	10.18
α_{20}	97.54	149.8	361.57
α_{21}	104.55	153.8	363.13

The curves of Figure 7 show that the system tends to be oscillatory at three separate and distinct frequencies. The lowest-frequency oscillation, with a period of about 0.3 second, appears on each curve. This oscillation indicates the degree of stability of the entire system, including the manifold, compressor, rotor dynamics, surge sensor, and blow-off valve. The higher-frequency oscillation, which appears also on all of the curves but is most predominant on the curve for ΔP_C, is caused by an oscillation of the moving element in the blow-off valve. The existence of the unstable conditions which produce this oscillation is shown mathematically in Appendix A. Its period is about 0.013 second, corresponding to a frequency of about 80 cycles per second.

The third oscillation, which is even higher in frequency, may be seen on the first part of the curve for ΔP_B. It is caused by vibration of the valve in the surge sensor, and it dies out after about 0.1 second because of the damping action of orifices A and A_o.

Although the system response after about one-half second is masked by the oscillation of the blow-off valve, the response for about the first 0.2 second is valid in Figure 7. Since ΔW_L is not one of the variables recorded, the step decrease in W_L does not appear in the figure, but its effect in decreasing W_a appears as a step decrease of about 0.25 pound per second in W_a at the beginning of the top curve. The decrease in W_a is not as great as the decrease in W_L because the increased compressor outlet pressure causes the air flow through the duct to increase immediately, and thus partly cancels out the effect of the step decrease. The action of the surge sensor in controlling the blow-off valve is governed by various time constants, so ΔW_a is not returned to zero until about 0.1 second after application of the step. Because of the time constants the control causes ΔW_a to overshoot the zero value and to reach a positive peak at about 0.17 second. Then, ΔW_a decreases again, and the curve for W_a would show a gradual convergence to zero, if the high frequency oscillation of the blow-off valve were not present. A better understanding of the curves and of the system may be gained by examining the status of the variables at various points along the time scale in Figure 7.

When t = 0, the step decrease of W_L has caused a momentary increase of P_3 of about 0.3 psia. This produces excessive force on the blow-off valve. Because of the valve's inertia, it does not open immediately, but the time constant is quite short and the valve is open about 0.03 inch after 0.04 second. Superimposed on this plot of y is the oscillation of the valve, which was started by the initial disturbance and is growing in amplitude exponentially.

The compressor air flow decreases by about 0.25 pound per second, as shown on the first curve of Figure 7. If all time constants which actually exist in the system had been simulated, the compressor air flow would have momentarily decreased by 1 pound per second, thus cor-

responding exactly to the decrease in W_L, and then it would have rapidly changed to the value shown in the curve, as the increased P_3 forced more air through the duct and effectively cancelled out part of the step decrease of W_L. This small pulse in the ΔW_a does not appear, because the very small time constants which would produce it were not included in the equations.

The step change in air-flow rate through the compressor initiates a high-frequency transient oscillation of the surge-sensor valve (variables Δx and ΔP_B).

The pressure in chamber C of the blow-off valve starts to rise because of the rise of Δy. Superimposed on this pressure is the waveform due to the oscillation of y.

The surge sensor valve displacement (Δx), the rotor-speed change (ΔN), and the manifold-pressure change (ΔP_M) start to rise. The pressure in chamber B of the surge sensor also starts to increase due to the increasing of Δx.

When t = 0.1 second, starting with the first curve, the change in compressor air flow, ΔW_a, has returned to zero because of the corrective action of the surge control, but ΔW_a is still increasing because of interaction of lags in the system.

The surge-sensor valve has reached a peak in its opening, as shown by the maximum for Δx.

The blow-off valve opening, as shown by the curve for Δy, is still increasing because the air flows into and out of chamber C have not yet reached equilibrium.

The engine speed has increased because of the decreased load on the compressor, which resulted from the initial decrease in W_a.

The average pressure in chamber C reached a peak at about 0.05 second and is now decreasing because of air being exhausted through the surge sensor's poppet valve.

The manifold pressure, P_M, is decreasing, after having just reached a maximum. The cause of this behavior may be explained in terms of the behavior of P_3, since the manifold pressure variations follow the P_3 variations, with a slight phase lag.

The pressure in chamber B is behaving in a manner similar to that of the manifold pressure, since it also follows the P_3 variations, with variations due to changes in x superimposed. The transient oscillation because of vibration of the valve at the beginning of the run has disappeared, but the influence of the vibrations of the blow-off valve is beginning to appear in the curve for ΔP_B.

The compressor outlet pressure, P_3, has reached a peak and is decreasing because the blow-off valve opening is increasing.

At t = 0.3 second, the oscillation of the blow-off valve has grown to a sufficient magnitude to make the remaining parts of the curves invalid.

4.2. CASE 2 WITHOUT DAMPING

A set of curves obtained for case 2 (valves partly open) from the Sanborn recorder is shown in Figure 8(a). For this run, the paper drive on the recorder was operated at one-half of the speed used for Figure 7, but each time mark still equals 1/100 second, so the time scale is different. The total system operating time covered by this set of data is about 1.5 seconds.

The initial behavior of each variable is similar to that for case 1, but the system is now stable. The blow-off valve oscillation, or chatter, still occurs, but it dies out after about a second. The system itself is stable, but the stability is somewhat marginal, since several cycles of oscillation occur before the transients die out, and control systems are usually considered to operate satisfactorily if they produce only one small overshoot when they are subjected to a step change of a controlled variable.

4.3. CASE 3 WITHOUT DAMPING

Results obtained from the simulation of case 3 (valves well open) are shown in Figure 8(b). Here, the oscillation of the blow-off valve is so small and of such short duration that it is no longer objectionable, but the system has become unstable. The low-frequency oscillations are growing rapidly in amplitude.

4.4. CASE 1 WITH DAMPING

In order to learn more about the nature of the blow-off valve oscillation, the computer circuit was modified to include viscous damping on the motion of the valve.

The results obtained when the viscous damping coefficient, K_f, was 0.0717 pound-second/inch are shown in Figure 9(a). The curves show that the damping retarded the rate of growth of the oscillation, but the oscillation still grew in amplitude. Hence, the damping was not of sufficient magnitude.

For Figure 9(b), the damping coefficient was raised to 0.1742 pound-second/inch. The curves show that with this amount of damping, the oscillation exponentially decays, but at a rather low rate.

In Figure 9(c) the K_f is 0.3584 pound-second/inch, and for Figure 9(d) it is 1.4336 pound-second/inch. In Figure 9(d), the oscillation is completely under control, and the transient dies out in a few cycles. Comparison of Figure 9(d) with other results for case 1 shows that addition of the damping had negligible effect on the system response, although it completely eliminated the valve chatter.

4.5. CASE 2 WITH DAMPING

The results of operation with values of K_f of 0.3584 pound-second/inch, 0.7168 pound-second/inch, and 1.4336 pound-second/inch are shown in Figure 10. Comparison of these

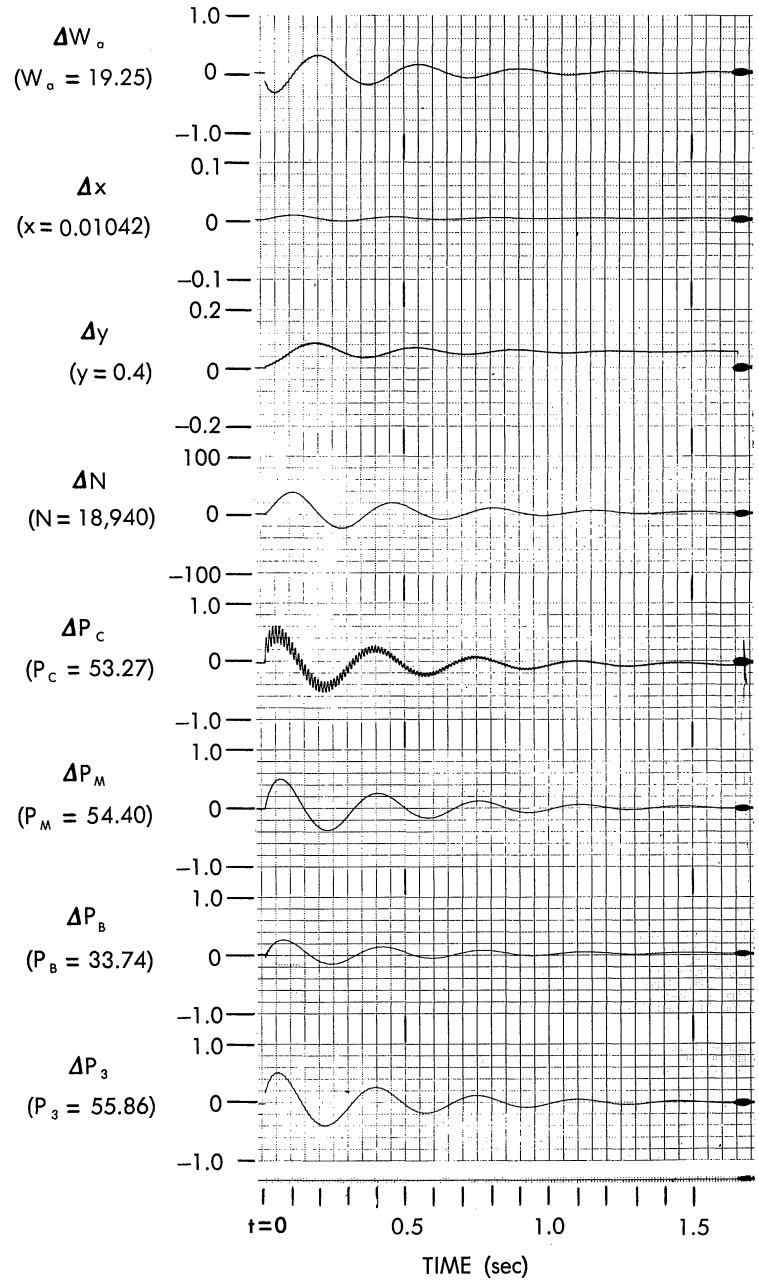

(a) Case 2

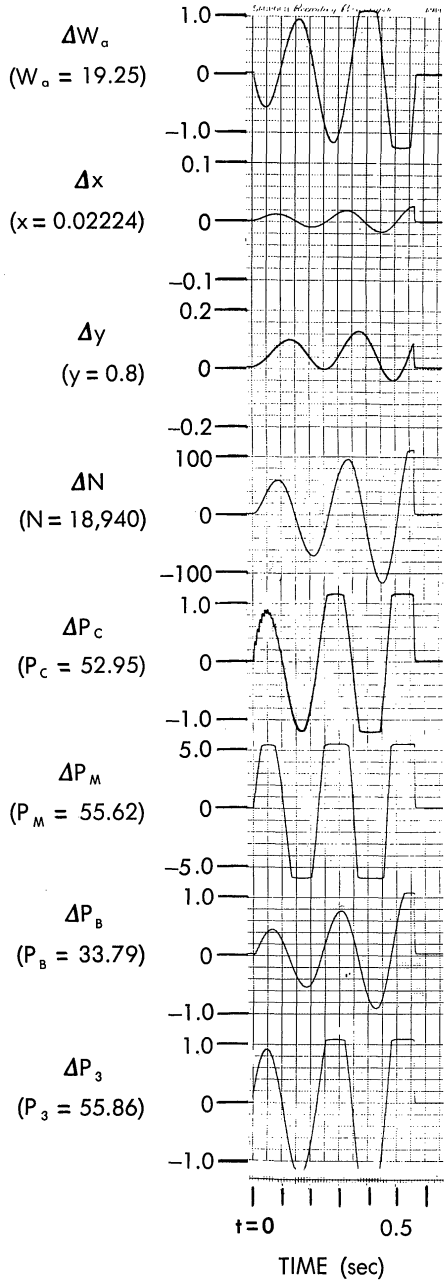

(b) Case 3

FIGURE 8. CASES 2 AND 3 WITHOUT DAMPING

runs with Figure 8(a) shows that the system response under "valve-open" conditions is not affected by the addition of viscous damping to suppress the high-frequency blow-off valve oscillations.

4.6. CASE 2 WITHOUT DAMPING, SPRING REMOVED FROM SURGE SENSOR

The results of an investigation of possible stabilizing effects of the springs in the surge sensor and blow-off valve are shown in Figure 11. Four sets of curves are shown in this figure. All four sets were obtained for case 2, and for zero damping ($K_f = 0$). For Figure 11(a), the surge-sensor spring constant, K_x, was set to zero. For Figure 11(b), normal values for both K_x and K_y were included. For Figure 11(c), the blow-off valve spring constant, K_y, was set equal to zero, and for Figure 11(d), both K_x and K_y were zero. Since the runs seem to be identical, it appears that eliminating the specified spring constants does not appreciably affect the operation of the system.

4.7. CASES 1 AND 2 WITH PISTON

A number of computer runs were made for a piston substituted for the diaphragm in the blow-off valve. Two changes in the analog computer diagram were made in order to include the piston simulation. First, an additional air-flow term, corresponding to the leakage between the piston and cylinder wall, was required in the gas-law equation for chamber C of the blow-off valve. Second, the coulomb friction force between the piston and cylinder walls became a term in the force-balance equation of the blow-off valve. The actual method of adding these features to the computer diagram is described in Section 3.3 of this report.

Since the magnitude of the coulomb friction force depends only upon the direction of motion of the piston and not upon its velocity, the introduction of the coulomb friction term made the simulator's operation nonlinear. Thus, the earlier statements concerning interpretation of magnitudes of variables on the computer data for the linear system do not apply for the system with coulomb friction. Thus, if the initial step in W_L is specified as 1 pound per second, the coulomb friction force (say 90 pounds) must be scaled to conform to this limitation, and the resulting curves are for a 1 pound per second change in W_L.

With proper precautions, however, certain interpretations can be made. If the same curves were regarded as results for a step of 0.1 pound per second in W_L, the ranges would decrease by a factor of 10, and the coulomb friction would increase by the same factor. The leakage area would remain the same, so the results would then be for a 0.1 pound air-weight flow decrease and coulomb friction of ±900 lbs, with ranges of 1/10 of those specified on the scales for the data.

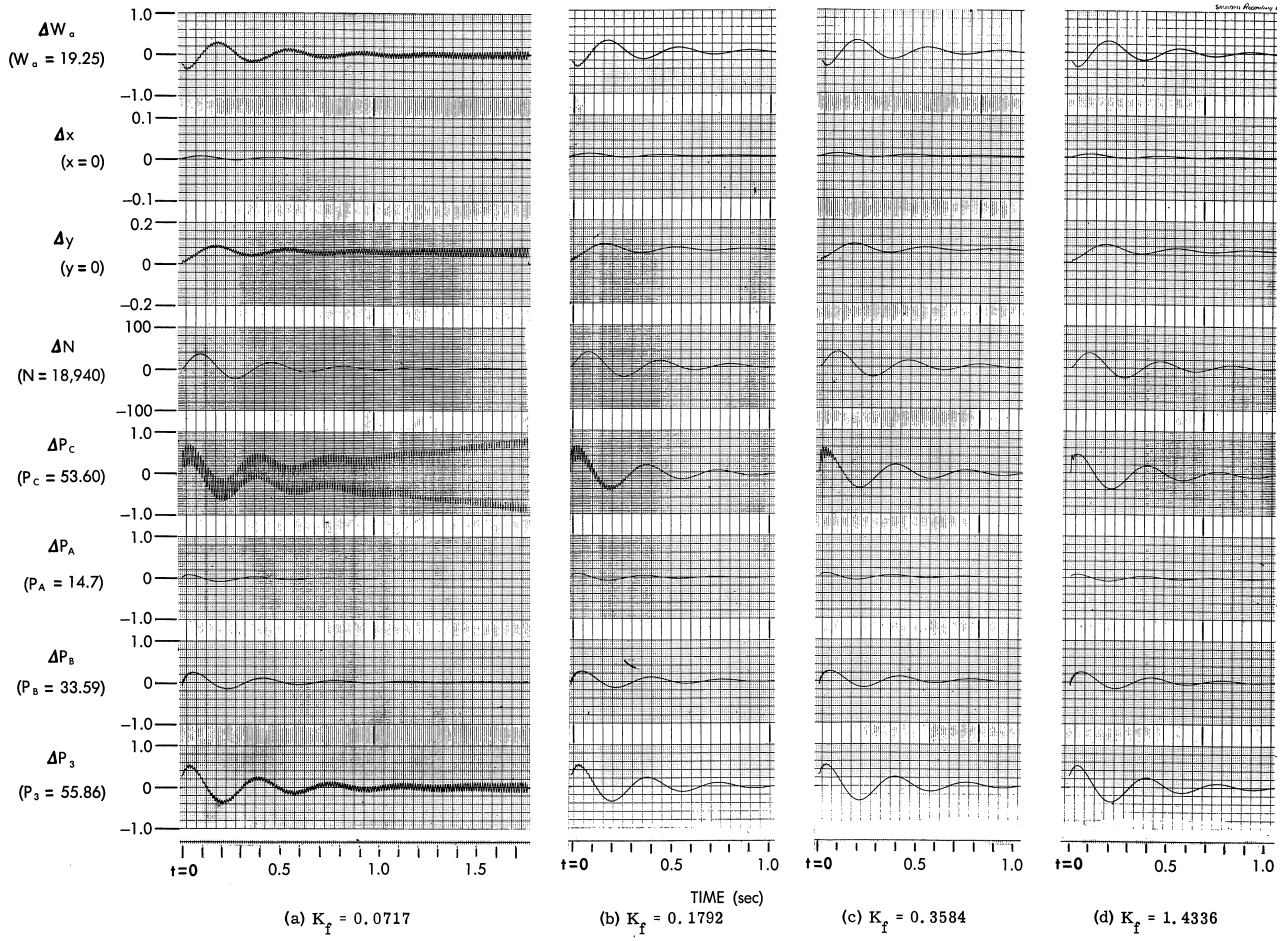

(a) $K_f = 0.0717$ (b) $K_f = 0.1792$ (c) $K_f = 0.3584$ (d) $K_f = 1.4336$

FIGURE 9. CASE 1 WITH DAMPING

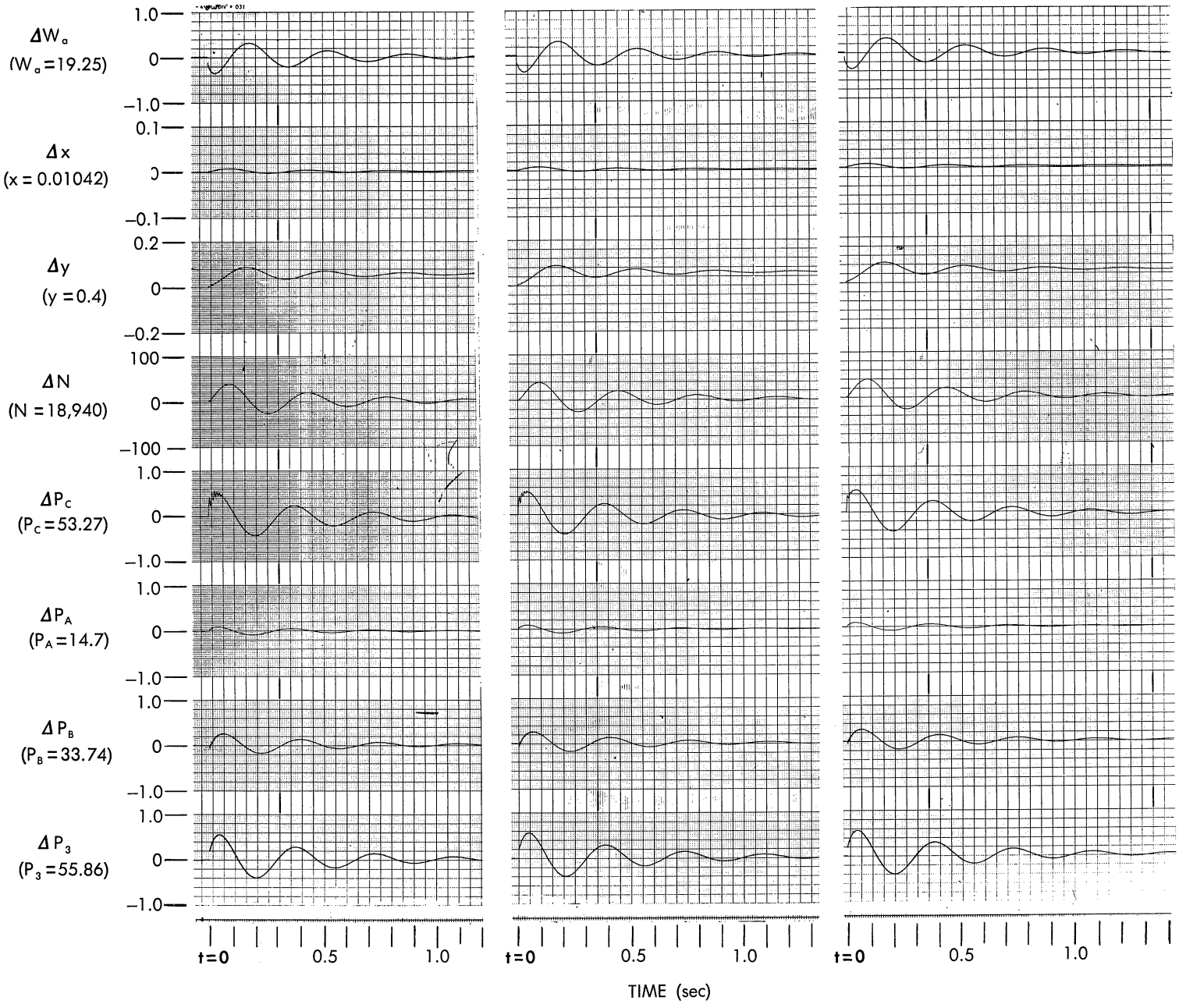

(a) $K_f = 0.3584$ (b) $K_f = 0.7168$ (c) $= K_f = 1.4336$

FIGURE 10. CASE 2 WITH DAMPING

3498-1-F

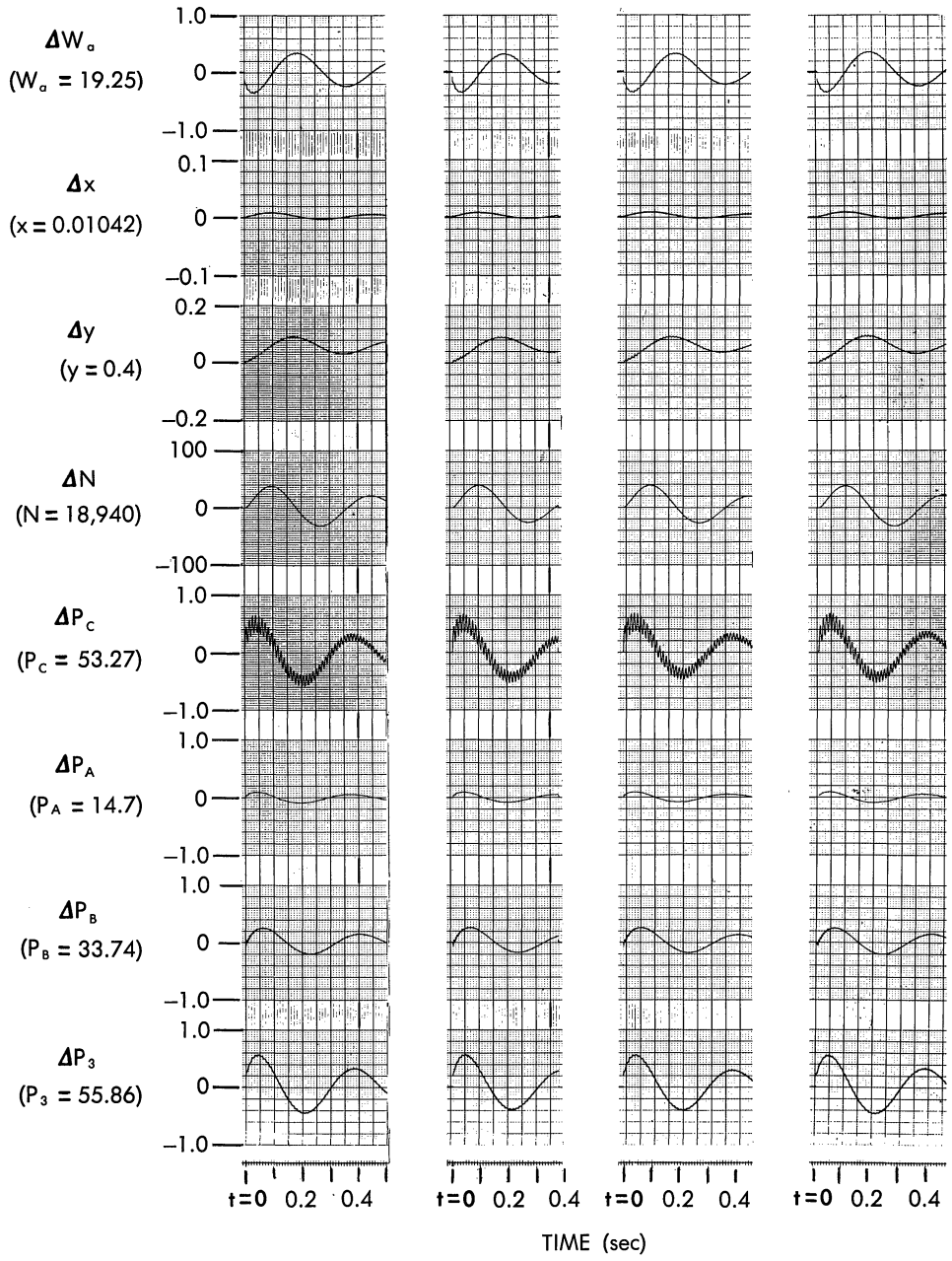

(a) $K_x = 0$ (b) Both Springs Included (c) $K_y = 0$ (d) $K_x = 0$, $K_y = 0$

FIGURE 11. EFFECTS OF SPRINGS ON SYSTEM OPERATION FOR CASE 2 WITHOUT DAMPING

Figures 12 through 16 are Sanborn recorder curves from the computer for cases 1 and 2 and pistons having various combinations of friction and air leakage. The parameters for the runs are listed in Table III.

TABLE III. COMPUTER RUNS OF THE SYSTEM WITH PISTON

Figure	Case	Friction	Leakage	ΔW_L (lb/sec)
12	1	90	0.009	1
13(a)	1	1	0.09	1
13(b)	1	1	0.360	1
13(c)	1	9	0.360	1
14	2	90	0.009	1
15	2	90	0.009	0.1
16	2	90	0.360	0.1

The runs show, in general, that the addition of the piston suppresses the chatter of the blow-off valve but is detrimental to the stability of the system itself. In fact, for large coulomb friction, the variables show a continuous nonsinusoidal oscillation after the original transient has died out.

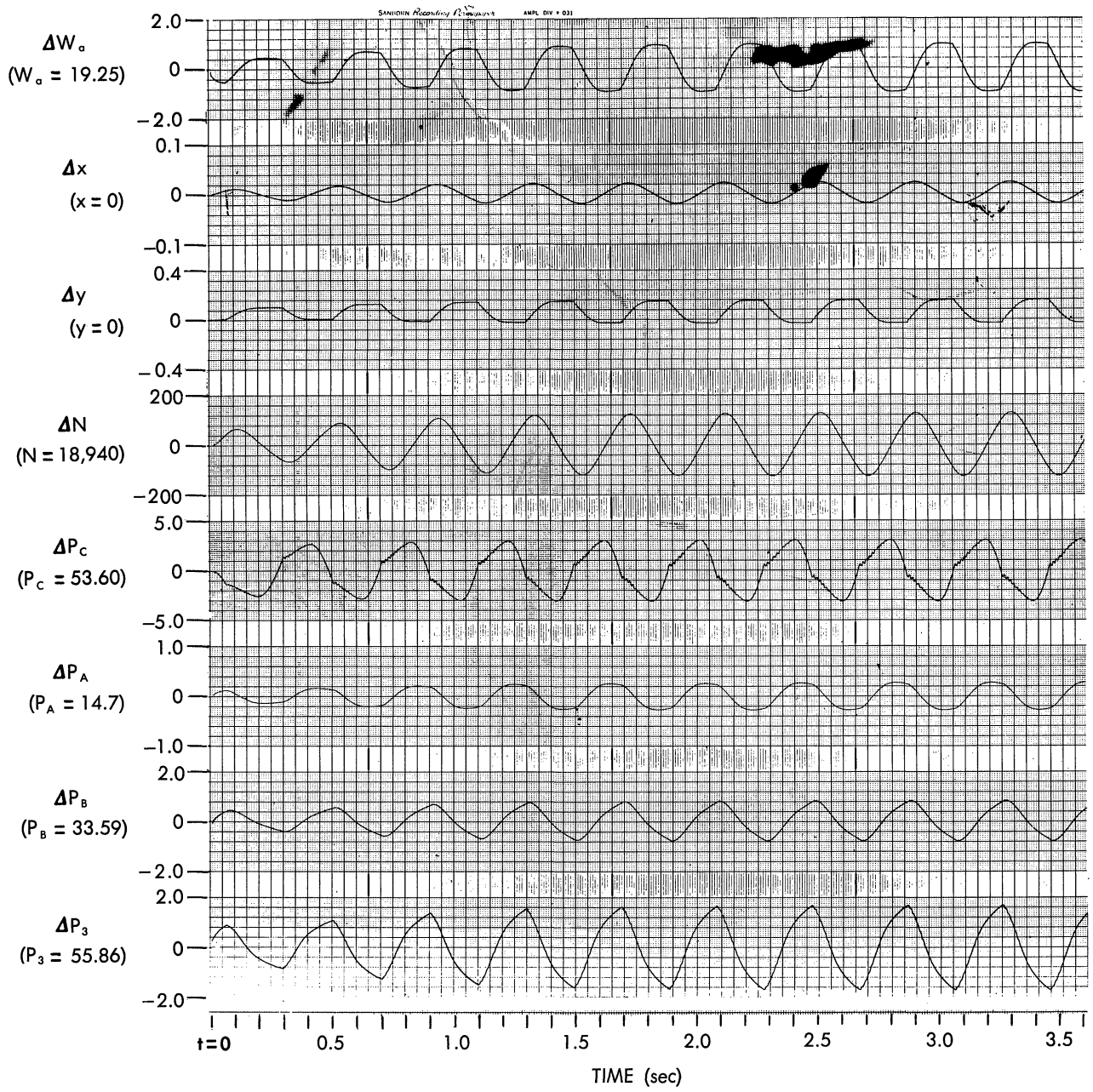

FIGURE 12. CASE 1 WITH PISTON. B = 90 lb, A = 0.009 in., W = 1 lb/sec.

3498-1-F

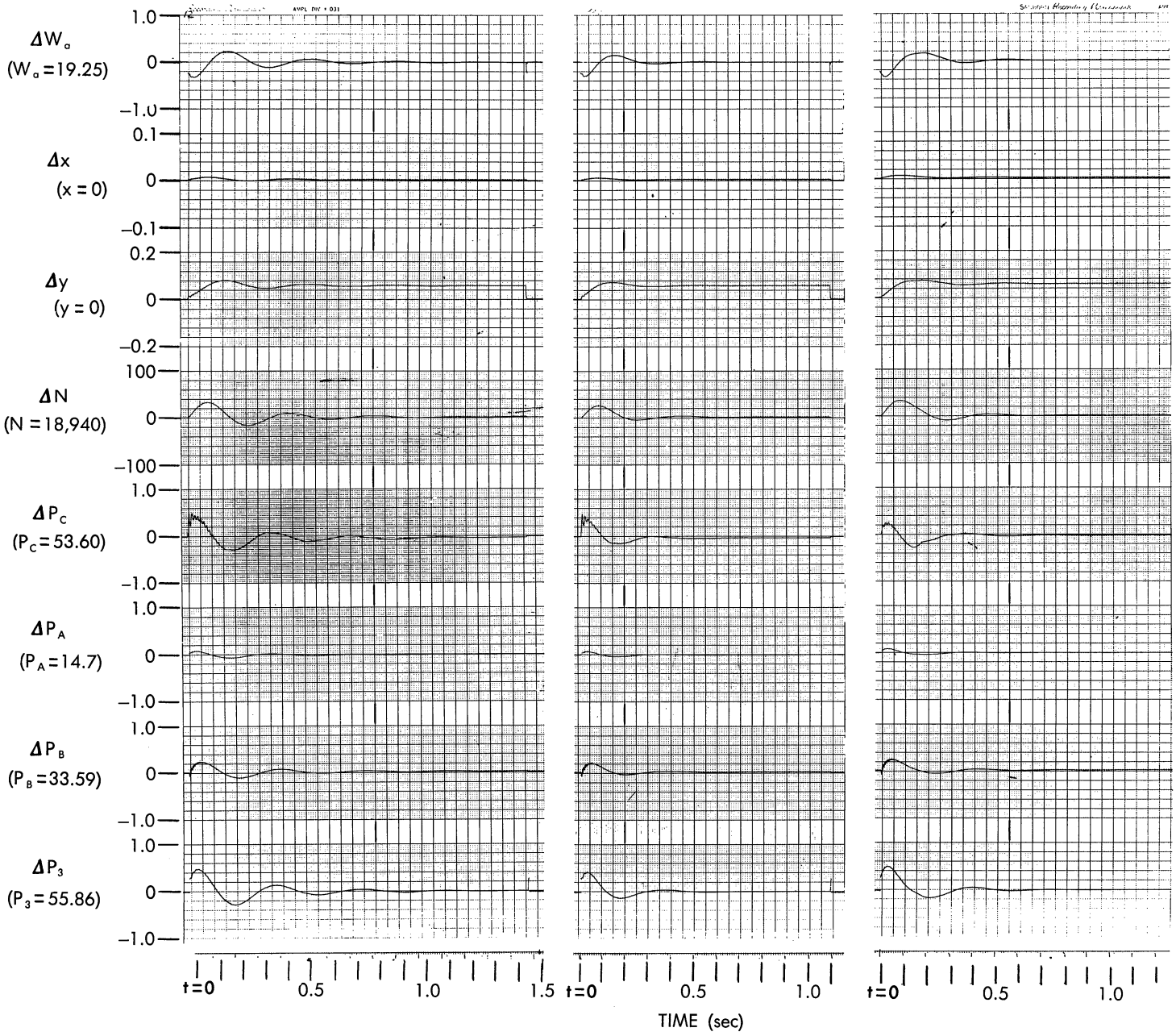

(a) B = 1, A = 0.09
W = 1

(b) B = 1, A = 0.360
W = 1

(c) B = 9, A = 0.360
W = 1

FIGURE 13. CASE 1 WITH PISTON. W = 1 lb/sec.

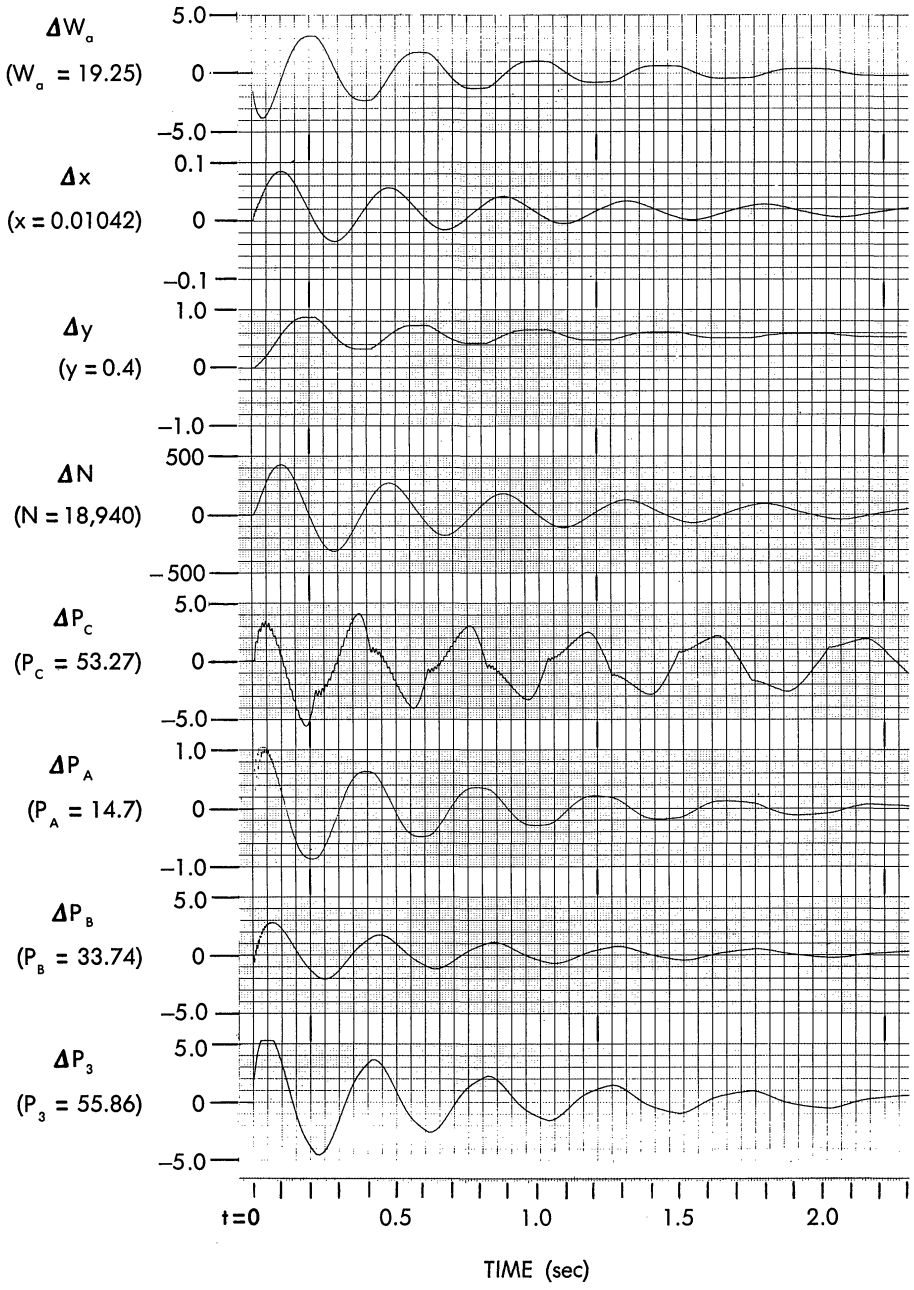

FIGURE 14. CASE 2 WITH PISTON. B = 90lb, A = 0.009 in., W = 1 lb/sec.

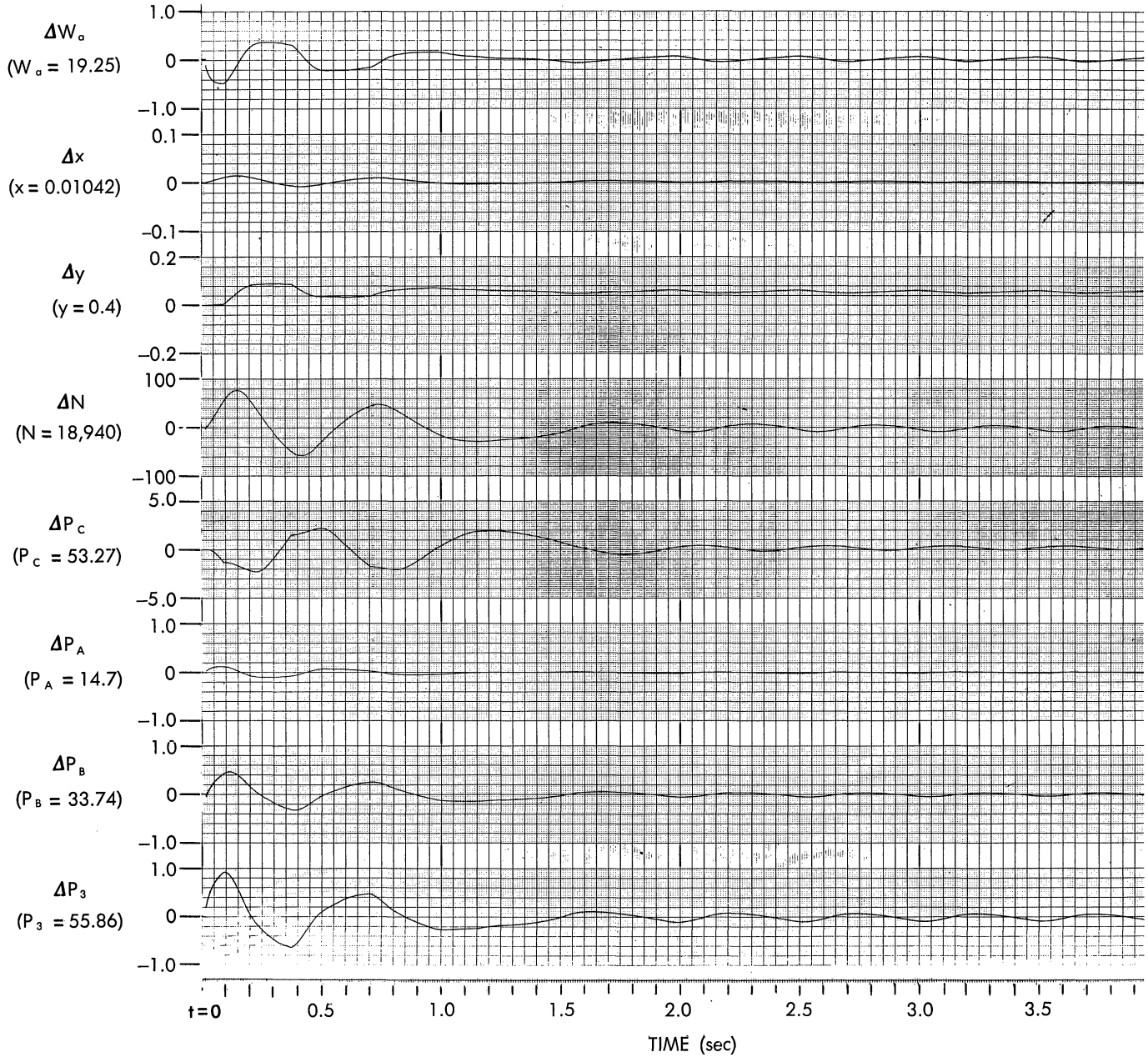

FIGURE 15. CASE 2 WITH PISTON. B = 90 lb, A = 0.009 in., W = 0.1 lb/sec.

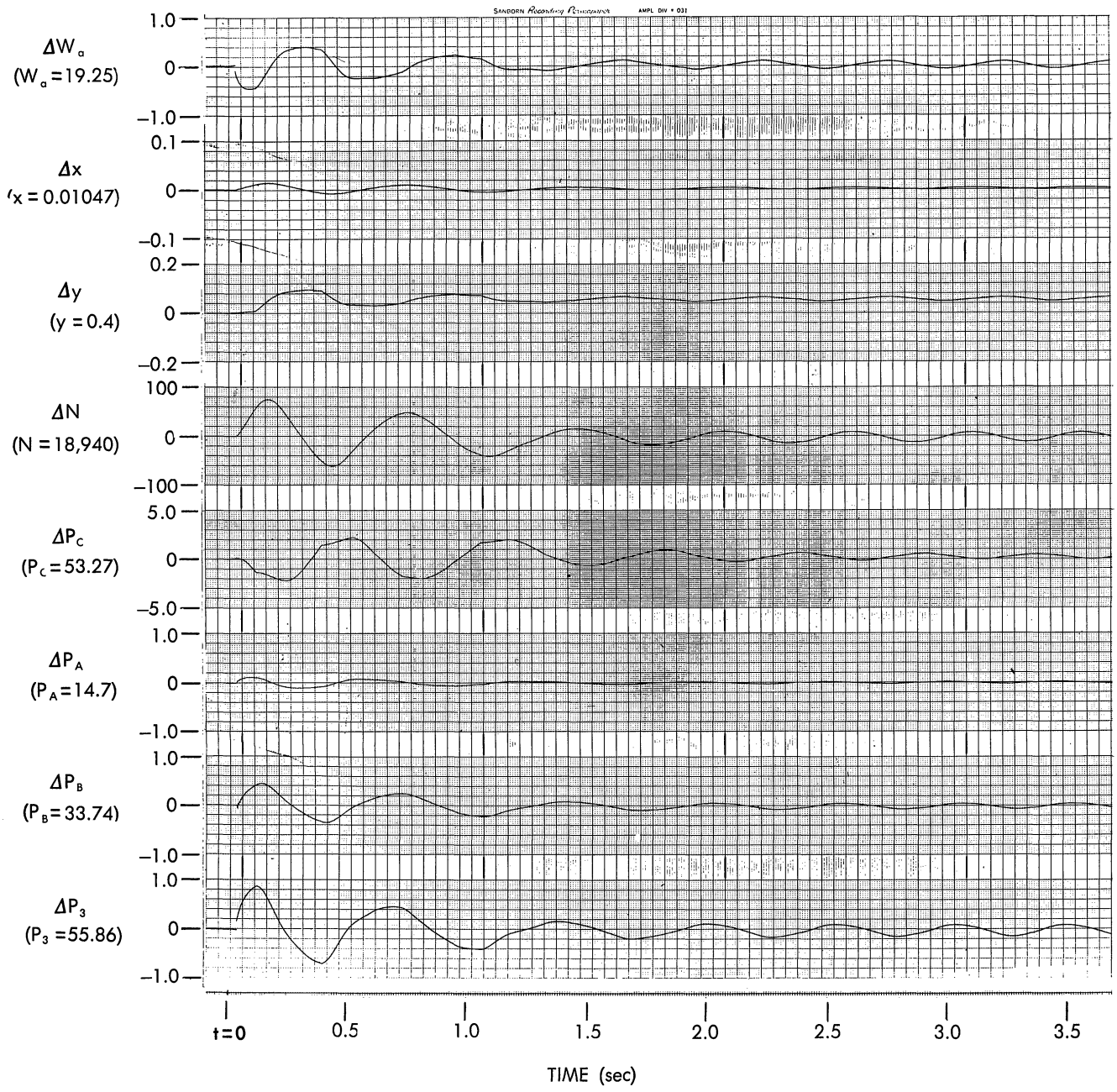

FIGURE 16. CASE 2 WITH PISTON. B = 90 lb, A = 0.360 in., W = 0.1 lb/sec.

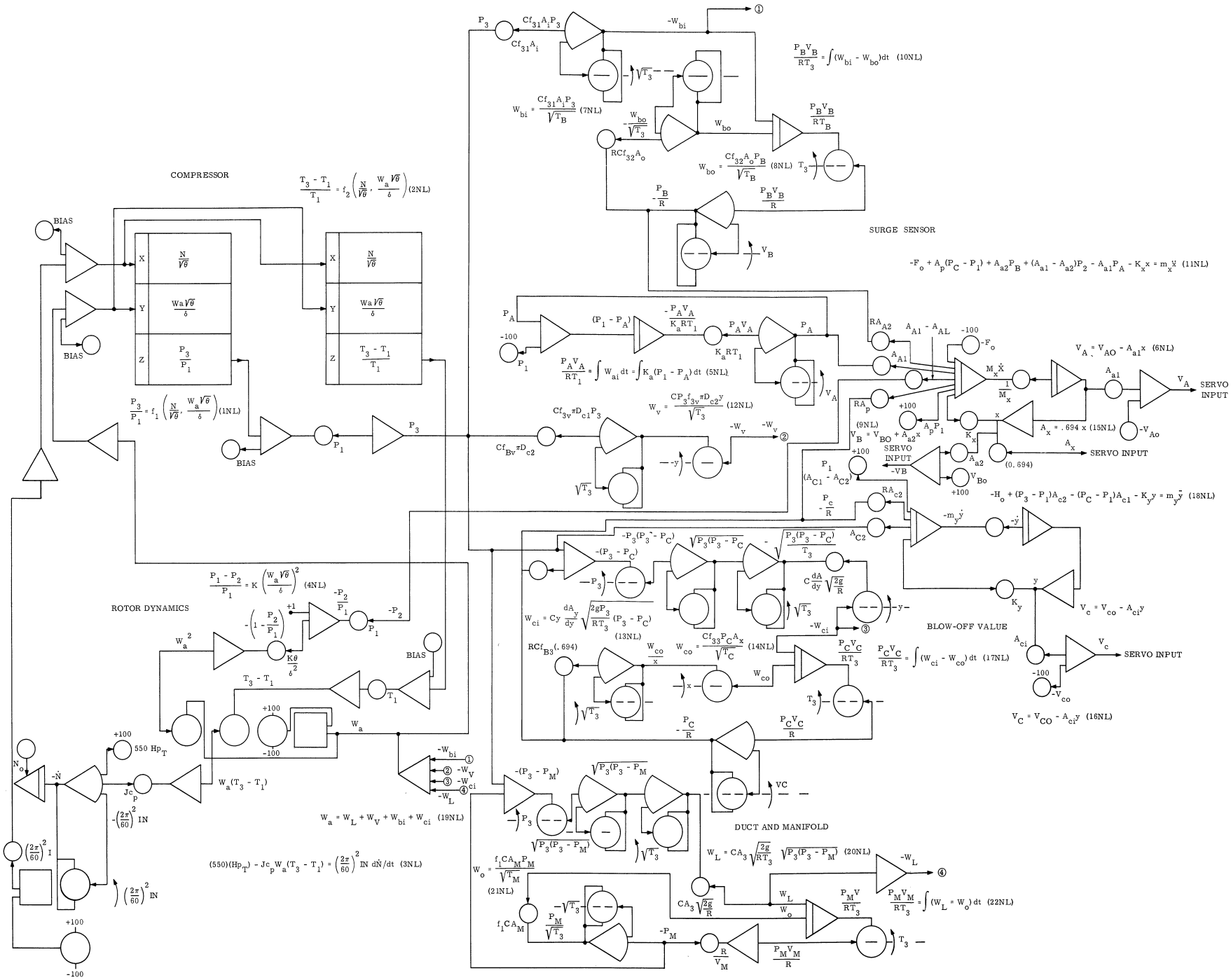

FIGURE 17. COMPUTER MECHANIZATION OF THE NONLINEAR EQUATIONS

5

ANALOG COMPUTER MECHANIZATION of NONLINEAR EQUATIONS

Figure 17 is a scaled diagram of a computer circuit for simulating the nonlinear equations of one compressor, its anti-surge control, the duct, and the manifold. It solves the nonlinear Equations 1NL through 22NL, which are listed in Section 2. The information flow diagram would be basically the same as Figure 5, except that the blocks would contain appropriate nonlinear equations, and the information flow lines would be labeled in terms of magnitudes of variables instead of increments.

Table IV gives the amount of analog computer equipment required.

TABLE IV. LIST OF ANALOG EQUIPMENT

No. of Units	Type of Analog Equipment
2	Function Generators of 2 Variables
13	Servo Multipliers (electromechanical, capable of 5 multiplications by the shaft variable)
9	Integrators
32	Amplifiers
37	Potentiometers

For this estimate, it was assumed that all flows through orifices were choked flows, and thus the flow parameters would be constants and therefore would not need to be generated as variables. It might be necessary to add some function generators to allow the simulation to operate for the complete range of variables. For example, the computation of air-weight flows in and out of chamber B of the surge control may require corrected air-weight flows as functions of the pressure ratios across this chamber's inlet and outlet orifices, and thus would require two function generators.

In Figure 17, the circuit which represents the compressor uses two function generators of functions of two variables in order to incorporate the compressor characteristics. These functions are $\frac{P_3}{P_1}$ as a function of $N/\sqrt{\theta}$ and $W\sqrt{\theta}/\delta$, and $\frac{T_3 - T_1}{T_1}$ as another function of the same two variables. The rotor dynamics computer uses two servo multipliers, with the shaft of one positioned by W_a and the shaft of the other positioned by $(2\pi/60^2)N$. In the diagram servo-driven multiplier potentiometers are labeled by the shaft variable written along with a curved arrow beside the potentiometer symbol. The multiplier potentiometers are represented by larger circles than those used as symbols for fixed coefficient potentiometers.

Appendix A

STABILITY of the BLOW-OFF VALVE

The computer results show the presence of exponentially-increasing oscillations of Δy for the case where the blow-off valve is nearly closed. If the simulation is changed to include a sufficiently large linear damping term in the force-balance equation for the blow-off valve, the resulting operation is stable. This damping term could be produced in the actual system by a dash pot attached to the moving part of the blow-off valve.

The following mathematical development verifies the instability of the system and demonstrates the effect of adding the dash pot. If the dash pot is included in the system, the equations for the blow-off valve are:

$$(P_3 - P_1)A_{c2} - (P_C - P_1)A_{c1} - K_y y = m_y \ddot{y} + K_f \dot{y}.$$

$$\frac{P_C V_C}{RT_C} = \int (W_{ci} - W_{co})\, dt.$$

$$W_{ci} = Cy \frac{dA_y}{dy} \sqrt{\frac{2gP_3(P_3 - P_C}{RT_3}}.$$

$$W_{co} = \frac{Cf_{33} P_C A_x}{\sqrt{T_3}}.$$

$$V_C = V_{CO} - A_{c1} y.$$

The first equation, in linearized form, is

$$A_{c2}\Delta P_3 - A_{c1}\Delta P_C - K_y \Delta y = m_y \Delta \ddot{y} + K_f \Delta \dot{y}. \qquad (1)$$

Substituting the last three equations into the second, differentiating with respect to time, and linearizing the resulting equation gives

$$\Delta\dot{P}_C = \alpha_{11}\Delta P_3 + \alpha_{12}\Delta y - \alpha_{13}\Delta P_C - \alpha_{14}\Delta A_x + \alpha_{15}\Delta\dot{y}, \tag{2}$$

where

$$\alpha_{11} = \frac{C_y \frac{dA_y}{dy}\sqrt{2gRT_3}(2P_3 - P_C)}{2\sqrt{P_3(P_3 - P_C)}}$$

$$\alpha_{12} = \frac{C \frac{dA_y}{dy}\sqrt{2gRT_3P_3(P_3 - P_C)}}{V_C}$$

$$\alpha_{13} = \frac{Cf_{33}A_x\sqrt{T_3}R}{V_C} + \frac{C_y \frac{dA_y}{dy}\sqrt{2gRT_3}P_3}{2V_C\sqrt{P_3(P_3 - P_C)}}$$

$$\alpha_{14} = \frac{Cf_{33}P_C\sqrt{T_3}R}{V_C}$$

$$\alpha_{15} = \frac{P_C A_{c1}}{V_C}$$

Assuming that the effects of ΔA_x and ΔP_3 do not appreciably contribute to the oscillatory behavior of the blow-off valve, the terms containing these quantities may be eliminated from Equations 1 and 2 to leave, from Equation 1:

$$-A_{c1}\Delta P_C - K_y\Delta y = m_y\Delta\ddot{y} + K_f\Delta y, \tag{3}$$

and, from Equation 2:

$$\Delta\dot{P}_C = \alpha_{12}\Delta y - \alpha_{13}\Delta P_C + \alpha_{15}\Delta\dot{y}. \tag{4}$$

Solving Equation 3 for $-\Delta P_C$, and differentiating with respect to time,

$$-\Delta\dot{P}_C = \frac{K_y}{A_{c1}}\Delta\dot{y} + \frac{K_f}{A_{c1}}\Delta\ddot{y} + \frac{m_y}{A_{c1}}\Delta\dddot{y}.$$

Substituting this expression for $-\Delta\dot{P}_C$ into Equation 4 gives

$$-\frac{K_y}{A_{c1}}\Delta\dot{y} - \frac{K_f}{A_{c1}}\Delta\ddot{y} - \frac{m_y}{A_{c1}}\Delta\dddot{y} = \alpha_{12}\Delta y + \alpha_{13}\left(\frac{K_y}{A_{c1}}\Delta y + \frac{K_f}{A_{c1}}\Delta\dot{y} + \frac{m_y}{A_{c1}}\Delta\ddot{y}\right) + \alpha_{15}\Delta\dot{y}.$$

Rearranging and multiplying by $\frac{A_{c1}}{m_y}$ gives

$$\Delta\dddot{y} + \left(\alpha_{13} + \frac{K_f}{m_y}\right)\Delta\ddot{y} + \left(\frac{\alpha_{13}K_f}{m_y} + \frac{\alpha_{15}A_{c1}}{m_y} + \frac{K_y}{m_y}\right)\Delta\dot{y} + \left(\frac{\alpha_{13}K_y}{m_y} + \frac{\alpha_{12}A_{c1}}{m_y}\right)\Delta y = 0. \qquad (5)$$

The characteristic equation for Equation 5 is of the form

$$p^3 + ap^2 + bp + c = 0.$$

Next, we apply a test to determine whether this equation has roots with positive real parts (the Hurwitz criterion) (Reference 3). Application of the mathematical algorithm for determination of the Hurwitz properties of polynominals leads to the following array.

$$\begin{array}{l}
\frac{1}{a}p \\
ap^2 + c\overline{)p^3 + bp} \\
\underline{p^3 + \frac{c}{a}p} \qquad \frac{a}{\left(b - \frac{c}{a}\right)}p \\
\left(b - \frac{c}{a}\right)p\overline{)ap^2 + c} \qquad \frac{\left(b - \frac{c}{a}\right)p}{c} \\
\underline{ap^2} \\
c\overline{)\left(b - \frac{c}{a}\right)p} \\
\underline{\left(b - \frac{c}{a}\right)p}
\end{array}$$

For stability, $\left(b - \frac{c}{a}\right) > 0$ (References 3 and 4), or $b > \frac{c}{a}$.

In Equation 5,

$$a = \alpha_{13} + \frac{K_f}{m_y};$$

$$b = \frac{\alpha_{13}K_f}{m_y} + \frac{\alpha_{15}A_{c1}}{m_y} + \frac{K_y}{m_y};$$

$$c = \frac{\alpha_{13} K_y}{m_y} + \frac{\alpha_{12} A_{c1}}{m_y} ;$$

then the condition for stability is

$$\frac{\alpha_{13} K_f}{m_y} + \frac{\alpha_{15} A_{c1}}{m_y} + \frac{K_y}{m_y} > \frac{\frac{\alpha_{13} K_y}{m_y} + \frac{\alpha_{12} A_{c1}}{m_y}}{\alpha_{13} + \frac{K_f}{m_y}} . \tag{6}$$

If K_f is zero corresponding to no dash pot, the condition for stability is:

$$\frac{\alpha_{15} A_{c1}}{m_y} + \frac{K_y}{m_y} > \frac{\frac{\alpha_{13} K_y}{m_y} + \frac{\alpha_{12} A_{c1}}{m_y}}{\alpha_{13}} ,$$

which simplifies, through algebraic manipulation, to:

$$\alpha_{15} > \frac{\alpha_{12}}{\alpha_{13}} .$$

Substituting for α_{15}, α_{12}, and α_{13} gives

$$\frac{P_C A_{c1}}{V_C} > \frac{C \frac{dA_y}{dy} \sqrt{\frac{2g}{RT_3}} P_3 (P_3 - P_C)}{\frac{Cf_{33} A_x}{\sqrt{T_3}} + \frac{Cy \frac{dA_y}{dy} \sqrt{\frac{2g}{RT_3}} P_3}{2\sqrt{P_3 (P_3 - P_C)}}} , \tag{7}$$

where $A_x = 0.694\ x$.

For case 1, x = 0 and y = 0, thus making the denominator of the right side of Inequality 7 zero. Since the numerator is not zero, the right side of this inequality is infinite, while

the left side is finite. This means that without the damping action of the dash pot, it is impossible for the inequality to be satisfied and consequently for this part of the system to be stable for case 1.

If the valves are open, however, it is possible for the inequality to be satisfied. This is verified by the computer runs for case 3 in Section 4 of this report.

In order to determine the magnitude of K_f needed to provide stability for case 1, we examine Inequality 6 under the condition that x = 0 and y = 0.

Rewriting Inequality 6, with $\alpha_{13} = 0$,

$$\frac{\alpha_{15} A_{c1} + K_y}{m_y} > \frac{\alpha_{12} A_{c1}}{K_f},$$

or,

$$K_f > m_y \frac{\alpha_{12} A_{c1}}{\alpha_{15} A_{c1} + K_y}. \tag{8}$$

Thus, the blow-off valve is stable for case 1 for the values of K_f specified for Inequality 8, and since opening of the valve tends to increase the stability, it will be stable for cases 2 and 3 also.

Appendix B
DIGITAL COMPUTATION of OPERATING POINTS

The use of a digital computer for computing steady-state operating points is highly recommended for either a nonlinear or linearized analog computer study of a system such as the one described in this report.

Use of a digital computer in this manner permits many more steady-state points to be investigated in a linearized simulation, since the digital computer may be programmed to not only obtain the steady-state points but also to compute the coefficients of the linearized equations from the steady-state parameters.

Hand computation would then be necessary only to obtain the partial derivatives from the compressor map.

In the nonlinear simulation the steady-state operating points would be useful as check points on the analog computer.

Input data to the digital computer was P_1, T_1, δ, θ (based on the altitude specified) and P_3, T_3, W_a, N obtained from the compressor map. T_M was also an input. The digital program was written in GAT (Generalized Algebraic Translator) language (Reference 5), and the

digital computer was an IBM 650 computer. The digital computer program was written to incorporate the following procedure of computation and also to compute the α coefficients as defined in Section 3, except that it is assumed here that T_M is not equal to T_3.

1. The following quantities are specified:

   P_3, W_a, N, T_3, T_M, P_1, δ, θ, and T_1.

2. Calculate P_2 from $P_2 = P_1\left[1 - (4.08)10^{-4}\frac{W_a{}^2\theta}{\delta^2}\right]$.

3. Calculate P_B from $P_B = (0.5907)P_3$.

4. Calculate P_C, x, and y by trial and error from these 3 equations:

$$x = \frac{1}{6}(0.0768P_C + 0.601P_B + 6.459P_2 - 7.1368P_1);$$

$$y = \frac{8.6629079xP_C}{\sqrt{P_3(P_3 - P_C)}};$$

$$P_C = \frac{1}{40.72}(38.48P_3 + 2.24P_1 - 32.8y).$$

5. Calculate W_V from $W_V = \frac{9.3418399P_3y}{\sqrt{T_3}}$.

6. Calculate W_L from $W_L = W_a - W_V$.

7. Calculate P_M from $P_M = P_3 - \frac{(0.00066253671)W_L{}^2T_3}{P_3}$.

8. Calculate W_o from $W_o = \frac{22.55688\,P_M}{\sqrt{T_M}}$.

9. Calculate V_A from $V_A = 1.83 - (7.06)x$.

10. Calculate V_B from $V_B = 0.196 + (0.601)x$.

11. Calculate V_C from $V_C = 58.43464 - 40.72y$.

The values of the parameters for six operating points are shown in Table V.

TABLE V. OPERATING POINTS COMPUTED BY DIGITAL COMPUTER

Altitude (ft)	20,000		30,000			
Quantity	Point 1	Point 2	Point 3	Point 4	Point 5	Point 6
P_1	6.753	6.753	4.362	4.362	4.362	4.362
δ	0.4594	0.4594	0.2967	0.2967	0.2967	0.2967
θ	0.8604	0.8604	0.7917	0.7917	0.7917	0.7917
T_1	447.4	447.4	411.70	411.70	411.70	411.70
P_3	27.01	26.94	17.45	17.71	17.40	17.58
W_a	9.708	9.713	6.535	6.485	6.538	6.501
N	18385	18366	17636	17689	17618	17680
T_3	746.38	746.14	685.63	687.08	685.27	686.50
T_M	741.28	741.16	681.73	682.46	681.55	682.17
P_2	5.694	5.693	3.678	3.689	3.678	3.686
P_B	15.95	15.91	10.31	10.46	10.28	10.38
P_C	25.36	25.40	16.37	16.17	16.40	16.23
x	0.0203	0.0155	0.0135	0.0374	0.0102	0.0269
y	0.6669	0.5305	0.4417	1.003	0.3483	0.7766
W_V	6.160	4.888	2.750	6.333	2.163	4.868
W_L	3.549	4.825	3.785	0.1518	4.375	1.633
P_M	26.78	26.51	17.08	17.71	16.90	17.51
W_o	22.19	21.97	14.75	15.29	14.60	15.12
V_A	1.687	1.720	1.735	1.566	1.758	1.640
V_B	0.2082	0.2053	0.2041	0.2185	0.2021	0.2122
V_C	31.28	36.83	40.45	17.58	44.25	26.81

Appendix C
SIMULATION of a LONG MANIFOLD

One of the ultimate objectives of the original project was a simulation of a manifold driven by more than one compressor. A simulation of a manifold driven by four compressors would have been impractical because of the large amount of analog equipment which it would have required. In the complete BLC system, which has two compressors driving each end of the manifold, there are two basic types of interaction between the compressors. One type is the interaction between compressors at the same end of the manifold. Here, changes in pressure

due to a change in output air-flow rate from one compressor immediately affect the other compressor. The other type of interaction is between compressors at opposite ends of the manifold. It is felt that the system's operation may be explored adequately by first simulating two compressors operating into a manifold at stations which are adjacent to each other, and then simulating a system which has a compressor at each end of the manifold.

When compressors are passing air into opposite ends of the manifold there are time-delay effects involved. For example, a sudden increase of air-flow rate from the compressor at one end causes the pressure in the manifold at that end to rise, but this change in pressure does not appear at the other end of the manifold instantaneously. Instead it propagates down the length of the manifold at the speed of sound. Since the manifold length is 90 feet, this delay is on the order of 1/10 of a second. In addition, the rising pressure is somewhat attenuated in passing down the manifold because of losses due to friction of the air against the manifold walls, and pressure drops due to air lost through the exhaust orifices. One possible method of simulating the action of the pressure wave in traveling down the manifold would be to simulate a separate smaller manifold for each of the two compressors, and then to couple the pressures of the two manifolds together by suitable analog dead time or time-lag simulators. Further consideration shows, however, that this approach might not be feasible because analog circuits which simulate transport delays have certain limitations which might cause instability of an arrangement such as the one described above, while the manifold itself would be quite stable. The ideas described in the following paragraphs might be developed further to give a simple method of simulating a manifold with a compressor at either end.

First, consider the analogy between pneumatic systems and electrical systems: pressure may be considered as voltage, air-flow rate as current, $\frac{V}{RT}$ as capacitance for a chamber where $\frac{PV}{RT} = \int W\,dt$, the viscous drag of the air as resistance, and the inertia (mass of the air) as inductance (Reference 6).

Figure 18 shows how an electrical transmission line whose operation is analogous to that of the manifold might be developed. Figure 18(a) shows a schematic representation of a manifold with five exhaust orifices and with air entering each end. Limiting the number of exhaust orifices simplifies the explanation, but the principles developed in Figure 18 apply to a manifold with any number of exhaust orifices. If the air is considered to have no inertia and is incompressible, the electrical network of Figure 18(b) is the electrical analog of the manifold. The pressure at either end of the manifold is represented by voltages at either end of the network. Current through the series resistors is analogous to longitudinal air flow in the manifold, and current through the shunt conductances corresponds to air flow through the orifices.

3498-1-F

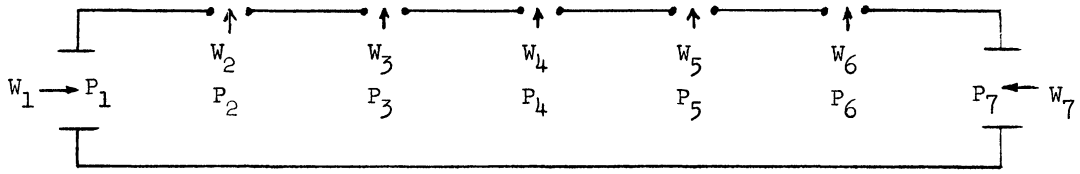

(a) Manifold with five orifices

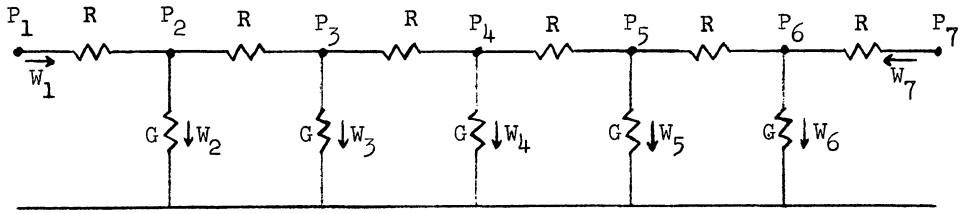

(b) Electrical network which is analogous to the manifold i-f inertial and compressibility effects of air are not considered

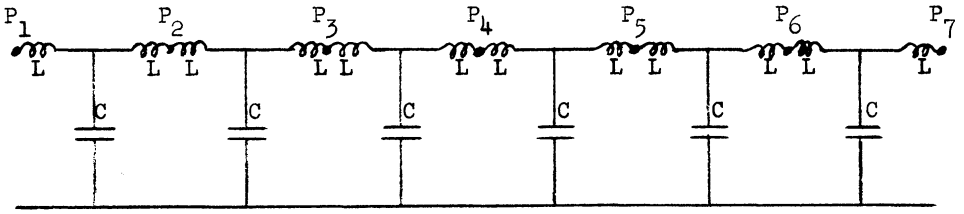

(c) Electrical network analogy for a manifold without air friction and without orifices

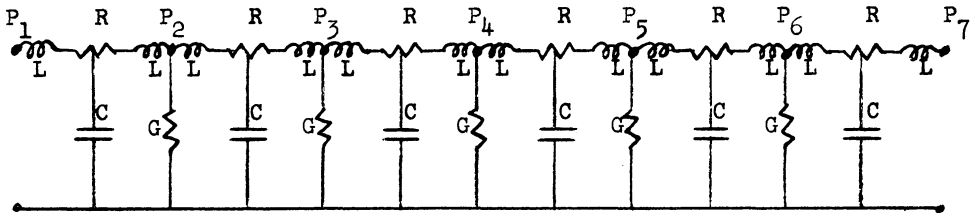

(d) Network analog for the manifold

FIGURE 18. DEVELOPMENT OF A NETWORK ANALOG FOR THE MANIFOLD

Voltage drops due to current in the series resistors correspond to pressure drops between adjacent orifices in the manifold resulting from friction of the air with the manifold walls.

Now consider the effects of air compressibility and inertia. Then examine the electrical analog of the manifold where these effects are present, but the orifices are closed, and friction of the air against the manifold walls is not considered. If the manifold is considered to be divided into six equal cylindrical volumes, each separate volume of air may be considered to have a certain mass and also to act as a spring. The electrical analog of a mass is an inductance, and the electrical analog of a spring is a capacitor. Thus, electrically, each of these

six sections may be represented by a series inductance and a shunt capacitance; and when the sections are combined, the electrical network shown in Figure 18(c) is the result. This network corresponds to a lumped-parameter electrical transmission line with no losses. Actually, since the air in the manifold could be divided into an infinite number of sections and each section would have mass and compressibility, the correct electrical analogy for the manifold would be a distributed parameter transmission line instead of the network shown in Figure 18(c). It is probable, however, that the lumped-parameter transmission-line analogy would be adequate. Further investigation would be needed to determine the number of stations required.

Figure 18(d) results from combining Figures 18(b) and 18(c). It may be recognized as a general lumped-parameter transmission line. The behavior of networks of this type has been extensively investigated, and complete mathematical descriptions of this behavior are available.

The transmission line may be simulated on the analog omputer by one of two methods. First, it may be possible to develop a transfer function for the generalized transmission line in terms of relationships between variables at its ends, and to use an analog computer to simulate this transfer function. Such a transfer function would involve transport delay, but would also include attenuation, and it could probably be mechanized so that tendencies toward instability in the computer circuit would be eliminated.

The second method would involve writing an ordinary differential equation for each station in the transmission line, and setting up a computer circuit which would solve this resulting set of simultaneous linear ordinary differential equations. The advantage of the second method is that it permits measurement of air pressures and air-flow changes at intervals along the transmission line. Simulation by this second method would require a rather large computer set-up if further investigation showed that it was necessary to use a large number of stations in the simulation. The first method (the use of transfer functions) would not require a lumped-parameter transmission-line analogy and thus might be simpler and more accurate, providing the transfer function itself is not too difficult to simulate.

REFERENCES

1. Joseph H. Keenan and Joseph Kaye, Gas Tables, Wiley, New York, N. Y., 1948.
2. John K. Jackson, Transfer Functions of Anti-Surge Control, Report No. R-1088-1, Cosmodyne Corporation, Los Angeles, Calif., 31 August 1959.
3. Ernest A Guillemin, Mathematics of Circuit Analysis, Wiley, New York, N. Y., 1949, pp. 395-409.
4. Eric B. Pearson, Technology of Instrumentation, Van Nostrand, New York, N. Y., 1957, pp. 118-122.
5. R. Graham and B. Arden, The Generalized Algebraic Translator, Statistical and Computing Laboratory, The University of Michigan, Ann Arbor, Mich., April 1959.
6. Allan R. Catheron and John F. Taplin, "Pneumatic Components," in John G. Truxal (ed.), Control Engineers' Handbook, McGraw-Hill, New York, N. Y., 1958, Sec. 16, pp. 7-11.

3498-1-F

DISTRIBUTION

30 copies
(1 repro)

Continental Aviation and Engineering Corporation
12700 Kercheval Avenue
Detroit 15, Michigan
ATTN: J. E. O'Shea, Purchasing Agent

AD Div. 30/2

Willow Run Laboratories, U. of Michigan, Ann Arbor
ANALOG COMPUTER INVESTIGATION OF A BOUNDARY-LAYER CONTROL SYSTEM by Margaret M. Spencer and Paul S. Fancher. Jan 60. 55 p. incl. illus. 5 tables, 6 refs.
(Rept. no. 3498-1-F)
(Contract AF 33(600)-38666) Unclassified report

A limited study using an analog computer was performed to investigate the stability of a pneumatic system consisting of a gas-turbine-driven compressor operating into a manifold from which air was escaping through a number of orifices. Simulation of linearized equations which describe the transient operation of the system for small departures from steady-state operating conditions was completed, and results of this simulation are presented. The results from this incomplete study show that the system has strong tendencies toward instability. A circuit for simulating the general nonlinear equations for the system is also presented. The linear and nonlinear simulations are compared. Methods of simulating a system consisting of a long manifold with one compressor at each end are discussed.

(over)

UNCLASSIFIED

1. Boundary-layer control systems – Design
2. Boundary-layer control systems – Effectiveness
3. Boundary-layer control systems – Performance
4. Boundary-layer control systems – Simulation
5. Boundary-layer control systems – Test results
6. Mathematical computers – Analog computers

I. Spencer, Margaret M. and Fancher, Paul S.
II. Continental Aviation and Engineering Corporation
III. Prime Contract AF 33(600)-38666

Armed Services Technical Information Agency
UNCLASSIFIED

AD Div. 30/2

Willow Run Laboratories, U. of Michigan, Ann Arbor
ANALOG COMPUTER INVESTIGATION OF A BOUNDARY-LAYER CONTROL SYSTEM by Margaret M. Spencer and Paul S. Fancher. Jan 60. 55 p. incl. illus. 5 tables, 6 refs.
(Rept. no. 3498-1-F)
(Contract AF 33(600)-38666) Unclassified report

A limited study using an analog computer was performed to investigate the stability of a pneumatic system consisting of a gas-turbine-driven compressor operating into a manifold from which air was escaping through a number of orifices. Simulation of linearized equations which describe the transient operation of the system for small departures from steady-state operating conditions was completed, and results of this simulation are presented. The results from this incomplete study show that the system has strong tendencies toward instability. A circuit for simulating the general nonlinear equations for the system is also presented. The linear and nonlinear simulations are compared. Methods of simulating a system consisting of a long manifold with one compressor at each end are discussed.

(over)

UNCLASSIFIED

1. Boundary-layer control systems – Design
2. Boundary-layer control systems – Effectiveness
3. Boundary-layer control systems – Performance
4. Boundary-layer control systems – Simulation
5. Boundary-layer control systems – Test results
6. Mathematical computers – Analog computers

I. Spencer, Margaret M. and Fancher, Paul S.
II. Continental Aviation and Engineering Corporation
III. Prime Contract AF 33(600)-38666

Armed Services Technical Information Agency
UNCLASSIFIED

AD Div. 30/2

Willow Run Laboratories, U. of Michigan, Ann Arbor
ANALOG COMPUTER INVESTIGATION OF A BOUNDARY-LAYER CONTROL SYSTEM by Margaret M. Spencer and Paul S. Fancher. Jan 60. 55 p. incl. illus. 5 tables, 6 refs.
(Rept. no. 3498-1-F)
(Contract AF 33(600)-38666) Unclassified report

A limited study using an analog computer was performed to investigate the stability of a pneumatic system consisting of a gas-turbine-driven compressor operating into a manifold from which air was escaping through a number of orifices. Simulation of linearized equations which describe the transient operation of the system for small departures from steady-state operating conditions was completed, and results of this simulation are presented. The results from this incomplete study show that the system has strong tendencies toward instability. A circuit for simulating the general nonlinear equations for the system is also presented. The linear and nonlinear simulations are compared. Methods of simulating a system consisting of a long manifold with one compressor at each end are discussed.

(over)

UNCLASSIFIED

1. Boundary-layer control systems – Design
2. Boundary-layer control systems – Effectiveness
3. Boundary-layer control systems – Performance
4. Boundary-layer control systems – Simulation
5. Boundary-layer control systems – Test results
6. Mathematical computers – Analog computers

I. Spencer, Margaret M. and Fancher, Paul S.
II. Continental Aviation and Engineering Corporation
III. Prime Contract AF 33(600)-38666

Armed Services Technical Information Agency
UNCLASSIFIED

AD Div. 30/2

Willow Run Laboratories, U. of Michigan, Ann Arbor
ANALOG COMPUTER INVESTIGATION OF A BOUNDARY-LAYER CONTROL SYSTEM by Margaret M. Spencer and Paul S. Fancher. Jan 60. 55 p. incl. illus. 5 tables, 6 refs.
(Rept. no. 3498-1-F)
(Contract AF 33(600)-38666) Unclassified report

A limited study using an analog computer was performed to investigate the stability of a pneumatic system consisting of a gas-turbine-driven compressor operating into a manifold from which air was escaping through a number of orifices. Simulation of linearized equations which describe the transient operation of the system for small departures from steady-state operating conditions was completed, and results of this simulation are presented. The results from this incomplete study show that the system has strong tendencies toward instability. A circuit for simulating the general nonlinear equations for the system is also presented. The linear and nonlinear simulations are compared. Methods of simulating a system consisting of a long manifold with one compressor at each end are discussed.

(over)

UNCLASSIFIED

1. Boundary-layer control systems – Design
2. Boundary-layer control systems – Effectiveness
3. Boundary-layer control systems – Performance
4. Boundary-layer control systems – Simulation
5. Boundary-layer control systems – Test results
6. Mathematical computers – Analog computers

I. Spencer, Margaret M. and Fancher, Paul S.
II. Continental Aviation and Engineering Corporation
III. Prime Contract AF 33(600)-38666

Armed Services Technical Information Agency
UNCLASSIFIED

AD

UNCLASSIFIED

UNITERMS

Analog computer
Stability
Pneumatic system
Compressor
Manifold
Orifices
Simulation
Linearized equations
Steady-state
Instability
Nonlinear equations
System

UNCLASSIFIED

AD

UNCLASSIFIED

UNITERMS

Analog computer
Stability
Pneumatic system
Compressor
Manifold
Orifices
Simulation
Linearized equations
Steady-state
Instability
Nonlinear equations
System

UNCLASSIFIED

AD

UNCLASSIFIED

UNITERMS

Analog computer
Stability
Pneumatic system
Compressor
Manifold
Orifices
Simulation
Linearized equations
Steady-state
Instability
Nonlinear equations
System

UNCLASSIFIED

AD

UNCLASSIFIED

UNITERMS

Analog computer
Stability
Pneumatic system
Compressor
Manifold
Orifices
Simulation
Linearized equations
Steady-state
Instability
Nonlinear equations
System

UNCLASSIFIED

AD Div. 30/2

Willow Run Laboratories, U. of Michigan, Ann Arbor
ANALOG COMPUTER INVESTIGATION OF A BOUNDARY-LAYER CONTROL SYSTEM by Margaret M.Spencer and Paul S. Fancher. Jan 60. 55 p. incl. illus. 5 tables, 6 refs.
(Rept. no. 3498-1-F)
(Contract AF 33(600)-38666) Unclassified report

A limited study using an analog computer was performed to investigate the stability of a pneumatic system consisting of a gas-turbine-driven compressor operating into a manifold from which air was escaping through a number of orifices. Simulation of linearized equations which describe the transient operation of the system for small departures from steady-state operating conditions was completed, and results of this simulation are presented. The results from this incomplete study show that the system has strong tendencies toward instability. A circuit for simulating the general nonlinear equations for the system is also presented. The linear and nonlinear simulations are compared. Methods of simulating a system consisting of a long manifold with one compressor at each end are discussed.

(over)

UNCLASSIFIED

1. Boundary-layer control systems – Design
2. Boundary-layer control systems – Effectiveness
3. Boundary-layer control systems – Performance
4. Boundary-layer control systems – Simulation
5. Boundary-layer control systems – Test results
6. Mathematical computers – Analog computers

I. Spencer, Margaret M. and Fancher, Paul S.
II. Continental Aviation and Engineering Corporation
III. Prime Contract AF 33(600)-38666

Armed Services Technical Information Agency
UNCLASSIFIED

AD Div. 30/2

Willow Run Laboratories, U. of Michigan, Ann Arbor
ANALOG COMPUTER INVESTIGATION OF A BOUNDARY-LAYER CONTROL SYSTEM by Margaret M.Spencer and Paul S. Fancher. Jan 60. 55 p. incl. illus. 5 tables, 6 refs.
(Rept. no. 3498-1-F)
(Contract AF 33(600)-38666) Unclassified report

A limited study using an analog computer was performed to investigate the stability of a pneumatic system consisting of a gas-turbine-driven compressor operating into a manifold from which air was escaping through a number of orifices. Simulation of linearized equations which describe the transient operation of the system for small departures from steady-state operating conditions was completed, and results of this simulation are presented. The results from this incomplete study show that the system has strong tendencies toward instability. A circuit for simulating the general nonlinear equations for the system is also presented. The linear and nonlinear simulations are compared. Methods of simulating a system consisting of a long manifold with one compressor at each end are discussed.

(over)

UNCLASSIFIED

1. Boundary-layer control systems – Design
2. Boundary-layer control systems – Effectiveness
3. Boundary-layer control systems – Performance
4. Boundary-layer control systems – Simulation
5. Boundary-layer control systems – Test results
6. Mathematical computers – Analog computers

I. Spencer, Margaret M. and Fancher, Paul S.
II. Continental Aviation and Engineering Corporation
III. Prime Contract AF 33(600)-38666

Armed Services Technical Information Agency
UNCLASSIFIED

AD Div. 30/2

Willow Run Laboratories, U. of Michigan, Ann Arbor
ANALOG COMPUTER INVESTIGATION OF A BOUNDARY-LAYER CONTROL SYSTEM by Margaret M.Spencer and Paul S. Fancher. Jan 60. 55 p. incl. illus. 5 tables, 6 refs.
(Rept. no. 3498-1-F)
(Contract AF 33(600)-38666) Unclassified report

A limited study using an analog computer was performed to investigate the stability of a pneumatic system consisting of a gas-turbine-driven compressor operating into a manifold from which air was escaping through a number of orifices. Simulation of linearized equations which describe the transient operation of the system for small departures from steady-state operating conditions was completed, and results of this simulation are presented. The results from this incomplete study show that the system has strong tendencies toward instability. A circuit for simulating the general nonlinear equations for the system is also presented. The linear and nonlinear simulations are compared. Methods of simulating a system consisting of a long manifold with one compressor at each end are discussed.

(over)

UNCLASSIFIED

1. Boundary-layer control systems – Design
2. Boundary-layer control systems – Effectiveness
3. Boundary-layer control systems – Performance
4. Boundary-layer control systems – Simulation
5. Boundary-layer control systems – Test results
6. Mathematical computers – Analog computers

I. Spencer, Margaret M. and Fancher, Paul S.
II. Continental Aviation and Engineering Corporation
III. Prime Contract AF 33(600)-38666

Armed Services Technical Information Agency
UNCLASSIFIED

AD Div. 30/2

Willow Run Laboratories, U. of Michigan, Ann Arbor
ANALOG COMPUTER INVESTIGATION OF A BOUNDARY-LAYER CONTROL SYSTEM by Margaret M.Spencer and Paul S. Fancher. Jan 60. 55 p. incl. illus. 5 tables, 6 refs.
(Rept. no. 3498-1-F)
(Contract AF 33(600)-38666) Unclassified report

A limited study using an analog computer was performed to investigate the stability of a pneumatic system consisting of a gas-turbine-driven compressor operating into a manifold from which air was escaping through a number of orifices. Simulation of linearized equations which describe the transient operation of the system for small departures from steady-state operating conditions was completed, and results of this simulation are presented. The results from this incomplete study show that the system has strong tendencies toward instability. A circuit for simulating the general nonlinear equations for the system is also presented. The linear and nonlinear simulations are compared. Methods of simulating a system consisting of a long manifold with one compressor at each end are discussed.

(over)

UNCLASSIFIED

1. Boundary-layer control systems – Design
2. Boundary-layer control systems – Effectiveness
3. Boundary-layer control systems – Performance
4. Boundary-layer control systems – Simulation
5. Boundary-layer control systems – Test results
6. Mathematical computers – Analog computers

I. Spencer, Margaret M. and Fancher, Paul S.
II. Continental Aviation and Engineering Corporation
III. Prime Contract AF 33(600)-38666

Armed Services Technical Information Agency
UNCLASSIFIED

AD

UNCLASSIFIED

UNITERMS

Analog computer
Stability
Pneumatic system
Compressor
Manifold
Orifices
Simulation
Linearized equations
Steady-state
Instability
Nonlinear equations
System

UNCLASSIFIED

AD

UNCLASSIFIED

UNITERMS

Analog computer
Stability
Pneumatic system
Compressor
Manifold
Orifices
Simulation
Linearized equations
Steady-state
Instability
Nonlinear equations
System

UNCLASSIFIED

AD

UNCLASSIFIED

UNITERMS

Analog computer
Stability
Pneumatic system
Compressor
Manifold
Orifices
Simulation
Linearized equations
Steady-state
Instability
Nonlinear equations
System

UNCLASSIFIED

AD

UNCLASSIFIED

UNITERMS

Analog computer
Stability
Pneumatic system
Compressor
Manifold
Orifices
Simulation
Linearized equations
Steady-state
Instability
Nonlinear equations
System

UNCLASSIFIED